ACKNOWLEDGMENTS

I would like to thank my supervisor at NTNU prof. Sigurd Skogestad for excellent help during my five months M. Sc.-study in Trondheim. I would also like to thank John Morud for his helpful advice and stimulating discussions. Thanks also to the students of the process control group for making my stay here at Norway a good time.

Last, but not least, I wish to express my appreciation of support and encouragement given by my supervisor at KTU doc. Saulius Kitrys and everybody from Department of Physical Chemistry.

Financial support from the State Educational Loan Fund of Norwegian Ministry of Church, Education and Research and from Joint Stock Company "ACHEMA" are gratefully acknowledged.

ABSTRACT

Chemical reactors, especially those in which rapid exothermic reactions take place, are often difficult to control. This is the case when wide fluctuations in temperature extremes result from relatively minor fluctuations in one or more operating variables. Operation in the unstable regions may result in poor product, runaway temperatures, rapid deterioration of the catalyst in packed reactors. Recognition of the circumstances which can cause such instability and knowledge of how to prevent it are important aspects of reactor design.

As chemical process plants become more efficient, they tend to become more tightly integrated, for example, raw materials are recycled and hot process streams are heat exchanged with cold process streams. This integration introduces tight couplings between processing units, which in some cases may make the dynamic and steady state behavior of the plant more complex, and lead to plants which are more difficult to operate and control.

This thesis work is concerned with the effect of feed-effluent preheating on the stability of industrial fixed bed ammonia and methanol synthesis reactors. Some of these reactors are examined. It is shown that reactors may exhibit limit cycle behavior (oscillations) at certain operating points. During such limit cycle behavior, reactors temperatures oscillate with amplitudes up to 100 ^{o}C, which is large enough to pose a potential threat to reactors.

ABSTRAKTAS

Contents

1 Introduction

1.1 Basis for the project

The starting point for this work was John Morud Ph.D. thesis "The Dynamics of Chemical Reactors with Heat Integration" (1995). In that work he analyzed a fixed bed industrial ammonia synthesis reactor, which became unstable. He used tabulated industrial data for the ammonia reaction rate as function of temperature and ammonia concentration. It is interesting to make analysis of stability of the ammonia synthesis reactor in general, using well-know reaction rate equations. The first goal of this project was to see if similar results could be obtained with a standard rate expression from literature.

The methanol synthesis process is carried out in fixed bed reactor like the ammonia synthesis reactor and both of them are very similar, especially their dynamic behavior. The second goal of this work was to see if similar unstable behavior could be found using a theorical analysis of a methanol synthesis reactor.

1.2 The aim of work and literature review

That chemical reactors sometimes go out of control is well known to those who are responsible for plant operation. Reactor stability and control have been an active research area for several decades. In spite of this, incidents such as reactor instability sometimes occurs in commercial plants. It is important to be able to predict such phenomena, as they may be fatal to a plant and hazardous to the plant personnel. Packed-bed reactors may display a rich range of steady state and dynamic behavior. Often, there is an economic incentive to operate near a region of parametrically sensitive behavior. In these regions, small changes in inlet conditions or physical parameters can lead to catastrophically large excursions in the bed temperature.

The performance under steady-state operating conditions of many fixed-bed reactors can be predicted quite well by calculations using mathematical reactor models, provided that the relevant data on the rates of the chemical and physical phenomena occurring in the reactor are known with adequate accuracy. By comparison, it may be more difficult to predict the transient behavior of reactor, in particular of fixed-beds catalytic reactors, because of the complicated interaction of heat and mass transport to and from catalyst particles, adsorption, desorption and chemical reaction. The development of satisfactory

dynamic models to describe such transient reactor behavior is important for a number of reasons:

— automation and optimizing control is being introduce in industry on an ever increasing scale;

— the optimum of reactor performance is often located near constraint boundaries imposed by e.g. the strength of construction materials, catalyst deactivation, safety considerations, optimization is only feasible when good dynamic models of reactors are available;

— the transient behavior of reactor should be known in sufficient detail for planning start-ups, shut-downs and changes in operating conditions caused by changes of feed or dictated by the necessity to vary product quality.

The main goal of this work is to investigate stability of the fixed bed ammonia and methanol synthesis reactors, based on a mathematical model analysis. The organization of the paper is as follows: first, a brief account is given of the diversity of industrially used ammonia and methanol process, because it is important to understand what processes take place inside synthesis loops and reactors. The following section presents a mathematical model of the ammonia or methanol synthesis reactors–describing the conservation of mass and energy. Simulations using this model reproduce the temperature oscillations observed in the industrial plants. Then it is performed a steady state analysis similar to that of van Herdeen (1953), which proves to be inadequate. Therefore it is proceeded with a linear dynamic analysis close to an operating point, which reveals that the instability occurs as a pair of conjugate poles cross the imaginary axis in the complex plane (Hopf bifurcation). The implications for operation and control of such reactors are discussed finally.

The rest of this Introduction is devoted to reviewing previous work. Maintaining operability and stability in the face of large process disturbances has always been a concern of engineering in process operation and general work on reactors stability, modelling and control is abundant. Crider and Foss (1968) refer to Nusselt (1927) and independently Schumann (1929) as the first to present a thermal analysis of packed beds. Van Herdeen (1953) and Aris and Amundson (1958) analysed the stability of the steady states of autothermal reactors. Orcutt and Lamb (1960), Baddour *et al.* (1965), and Luss and Amundson (1967) studied the stability of the autothermal system and gave insight to the operations problems, but did not provide strategies for responding to disturbances. Limit cycle behavior in autothermal reactors was presented

by Reilly and Schmitz (1966,1967) and Pareja and Reilly (1969). Stephens and Richards (1973) performed a steady state and dynamic analysis of an ammonia synthesis plant and notice that steady state stability criteria are not sufficient for stability. The fixed bed reactor is discussed extensively in the survey of Ray (1972) and the further survey of Schmitz (1975), Eigenberger (1976) and Jørgensen (1986). Vakil *et al.* (1973), Wallmann *et al.* (1979), Foss *et al.* (1980) and Wallman and Foss (1981) study the use of multivariable controllers for the control of fixed bed reactors. Silverstein and Shinnar (1982) discuss the stability of the heat integrated fixed bed reactor.

2 Ammonia and methanol synthesis

Ammonia and methanol are very important chemicals with a wide range of applications.

Ammonia is basicly used as fertilizer and for manufacturing other fetilizeres, such as ammonium nitrate, ammonium sulphate, urea and others. Ammonia can be also used for refrigeration processes as freezing agent.

Methanol is very widely used for manufacturing other chemicals, such as formaldehyde, dimethyl terephtalate, acetic acid, chloromethanes and others. More recently, methanol has been used as clean synthetic fuel. Methanol can be also converted to high octane gasoline.

2.1 Ammonia and methanol synthesis loops

Ammonia synthesis loop

As measured by sales volume, ammonia is the leading product of the entire petrochemical industry. By far the most important method of manufacturing ammonia is synthesis from the elements:

$$N_2 + 3H_2 \Leftrightarrow 2NH_3, \tag{1}$$

basicly using the Haber Bosch system; this accounts for over 90 % of world ammonia production. Today, variations of the Haber Bosch process differ less in the synthesis step than in synthesis gas preparation and purification. The equilibrium for the synthesis reaction is favorable to producing ammonia only at very low temperatures or very high pressures. Nevertheless, the known catalysts, based on Fe, permit achieving satisfactory reaction rates beginning at temperature about 300–350 ^oC. At the usual commercial reactor operating conditions, the conversion achieved per pass is only about 20–30 %. However, optimum conversions per pass are usually lower. In practically all commercial ammonia plants, the Haber Bosch recycle loop process is still used to make possible substantially complete conversion of the synthesis gas. In this system, following the reaction, the ammonia formed is removed from the gas, the uncorverted synthesis gas is supplemented with fresh make up gas, and the mixture fed again to the synthesis reactor (see Figure 1). A recycle compressor compensates for the unavoidable pressure drop that results from flowing the circulating gas through the equipment and piping. Almost exclusively, cooling the gas mixture below its ammonia dew point and withdrawing the condensed

liquid serves to recover ammonia from the recycle gas. Usually, the fresh make up gas contains small quantities of inert components, such as methane and argon, which concentrate in the synthesis loop. The concentration of inerts in the synthesis loop is controlled at the desire level by withdrawing a small side stream, the "purge gas".

Methanol synthesis loop

Methanol is produced on a large industrial scale from synthesis gas, a mixture of CO, CO_2 and H_2. The following chemical reactions take place (Graaf *et al.*, 1988):

$$CO + 2H_2 \Leftrightarrow CH_3OH \tag{2}$$

$$CO_2 + 3H_2 \Leftrightarrow CH_3OH + H_2O \tag{3}$$

$$CO_2 + H_2 \Leftrightarrow CO + H_2O \tag{4}$$

A high selectivity commercial $Cu/ZnO/Al_2O_3$ catalyst is used in modern units. The present methanol processes allow to produce 0.40 to 0.60 mole of methanol for each mole of methane used. The balance is used as energy supply to make the process feasible and operate compressors and distillation columns.

Ammonia and methanol synthesis processes are very similar because both processes need a high temperature and a high pressure and they belongs to the category of "autothermic processes". In these synthesis reactions the temperature is maintained by the heat of reaction alone. In order to achieve this conditions, gas flow and heat exchange are arranged to reduce the increase in temperature associated with the exothermic reaction and to suppress the need for an external source of heat once the reaction is started. Although several industrial reactor systems have been used for these processes (Zardi, 1982 and Dybkjaer, 1985), they have two principal characteristics in common. Firstly, the systems contain two-phase reactors in which the porous catalyst is the solid phase and the reaction mixture is gaseous phase. Secondly, the reactors are placed in a recycling system because the ammonia and methanol synthesis reactions presented above are limited by chemical equilibrium. Therefore the reactions mixtures are cooled after leaving reactors (ammonia or methanol and water). The unreacted remaining synthesis gas is then partly recycled to the reactor inlet. The reaction system for ammonia or methanol synthesis includes not only the reactor unit but ancillary equipment like cycle gas compressors,

heat exchangers or a boiler and separator– the equipment that may influence the design of the optimum reactor as well as be influenced by it. The ammonia

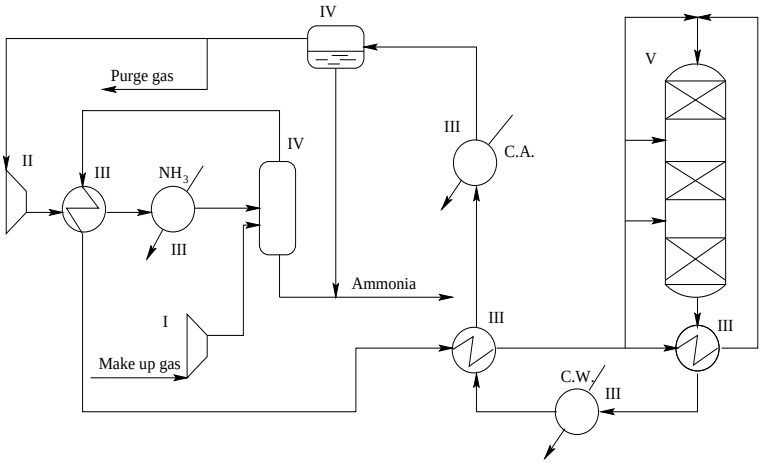

Figure 1: Ammonia synthesis loop with fixed-bed quench cooling reactor: I–make up gas compressor, II–circulator, III–heat exchanger, IV–separator, V–fixed bed ammonia reactor

or methanol reactor is of course the heart of the synthesis plant. The schemes of loops are shown in Figure 1 and Figure 2. Of course, they can be other configurations but these schemes are assumed as a basis in the current work.

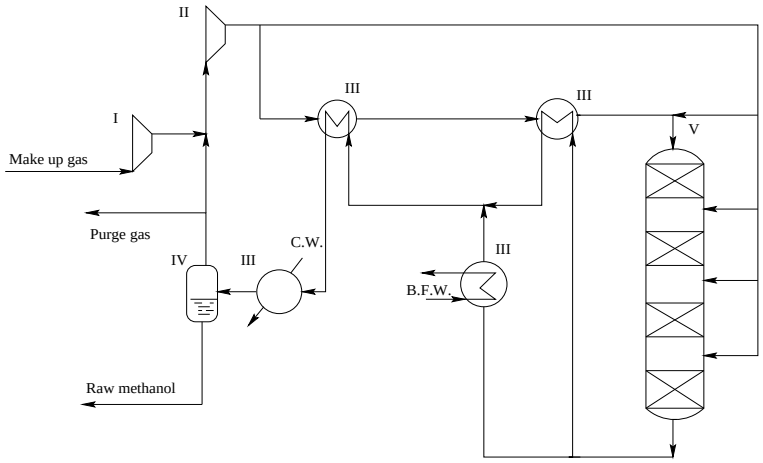

Figure 2: Methanol synthesis loop with fixed-bed quench cooling reactor: I–make up gas compressor, II–circulator, III–heat exchanger, IV–separator, V–fixed bed methanol reactor

As can be seen both schemes are very similar. The main difference is in kinetic

schemes.

2.2 Ammonia and methanol kinetic schemes

Knowledge of the macrokinetics is important for solving the industrial problem of designing ammonia and methanol synthesis reactors, for determining the optimal operating conditions, and for computer control of ammonia and methanol plants. This means predicting the technical dependence on operating variables of the rate of formation of ammonia or methanol in integral catalyst volume element of a converter.

An ammonia synthesis kinetic model

Since the beginning of commercial ammonia synthesis, a large number of different kinetic equations have been suggested, emanating in each case from a proposed reaction mechanism or from empirical evaluations. The first kinetic equation (Temkin and Pyzhev, 1940) useful for engineering proposes is well-know Temkin and Pyzhev reaction rate Equation 8. It is based, among other considerations, on the assumption that on an energetically inhomogeneous surface adsorbed nitrogen inhibits the slowest step of the reaction sequence, the adsorption of nitrogen. For many years, this formulation are the basic design equation for industrial ammonia reactors. Values for the factor α between 0.5 (Adams and Comings, 1953) and 0.75 (Temkin *at al.*, 1963) are used. For zero ammonia concentration, the equation gives infinitely large reaction rates; for this case, simpler relationship is said to apply(Equation 5) (Kiperman and Granovskaya, 1952).

$$v = k' \, p_{H_2}^{\alpha} p_{N_2}^{1-\alpha} \, . \tag{5}$$

In later years it could be demonstrated that Equation 8 are a simplified form of a more general model equation. For α=1, this may be derived from the concept of energetically homogeneous (Langmuir-Hinshelwood adsorption isotherm) as well as for heterogeneous surfaces (Elovich type of isotherm). The applicability of one equation or another depends on the reduction state of the catalyst (Ozaki *at al.*, 1960) or the promotor type (Aika and Ozaki, 1969). Equation 6 is a combination of these model equations.

$$v = \frac{k_{-1}^{0} \left(a_{N_2} \, K_a^2 - \frac{a_{NH_3}^2}{a_{H_2}^3} \right)}{\left(1 + K_3 \, \frac{a_{NH_3}}{a_{H_2}^w} \right)^{2\alpha}} \, , \tag{6}$$

where $w = 1.5$ and $\alpha = 0.75$.

Verification for a commercial catalyst confirmed the validity of this extended model, which transforms into Equation 8 near thermodynamic equilibrium (Nielsen, 1970). Another equation (Brill, 1970) may be regarded as a variant of Equation 6 also. The ICI (Imperial Chemical Industries, Ltd.) Laboratories tested an Equation 7 (ICI: Catalyst Handbook, 1970) over a wide range of operating conditions.

$$v = \frac{k\, p_{N_2}^{1-\alpha} \left(1 - \frac{p_{NH_3}^2}{K\, p_{N_2}\, p_{H_2}^3}\right)}{\left(\frac{1}{p_{H_2}} + \frac{p_{NH_3}^2}{K\, p_{N_2}\, p_{H_2}^3}\right)^{\alpha} \left(1 + \frac{1}{p_{H_2}}\right)^{1-\alpha}}. \tag{7}$$

For very small ammonia concentrations or at conditions far removed from equilibrium, Equation 7 becomes equivalent to Equation 5. For high operating pressures, it is equivalent to Equation 8. At this time, therefore, Equation 7 represents the most general rate equation for industrial ammonia synthesis. Although this, in the current work the Equation 8 is used in simulations of the ammonia reactor stability because there are high operating pressure and high ammonia inlet concentration. Reaction rates values, which were simulated by Equation 7, are not exactly the same like in industrial plant case (see Morud, 1995).

$$r_{N_2}\rho_{cat.} = k_1\, p_{N_2} \left(\frac{p_{H_2}^3}{p_{NH_3}^2}\right)^{\alpha} - k_{-1} \left(\frac{p_{NH_3}^2}{p_{H_2}^3}\right)^{1-\alpha}, \tag{8}$$

where $\alpha = 0.5$ and the parameter values are taken from Froment and Bischoff (1990):

$$k_1^o = 1.79 \times 10^4 \exp\left(-\frac{87\,090}{RT}\right) \tag{9}$$

and

$$k_{-1}^o = 2.57 \times 10^{16} \exp\left(-\frac{198\,464}{RT}\right). \tag{10}$$

In the current work these parameter values were multiplied by a factor $k = 4.75$, i.e. $k_1 = k\, k_1^o$ and $k_{-1} = k\, k_{-1}^o$. The coefficient k takes into account the differences in catalyst activity and it was adjusted to match the industrial data of Morud (1995).

A methanol synthesis kinetic model

The main lines in the mechanism of conversation of CO, CO_2 and H_2 feed into methanol over a $Cu/ZnO/Al_2O_3$ catalyst are now well established, and a large number of kinetic equations have been proposed.

Generally speaking, the mechanism can be based on three overall reactions (Equations: 2, 3, 4): the hydrogenations of CO_2 and CO, and the water gas shift reaction.

Early kinetic models were derived for the zinc chromite catalyst of the high pressure process, which has now almost completely been abandoned in favor of the low pressure technology. A classic example from this early work is the equation proposed by Natta (1955) for the ZnO/Cr_2O_3 catalyst:

$$r_{CH_3OH} = \frac{f_{CO}\, f_{H_2}^2 - \frac{f_{CH_3OH}}{K_2^{eq}}}{(A + B\, f_{CO} + C\, f_{H_2} + D\, f_{CH_3OH})^3}\,. \tag{11}$$

Apparently, Natta assumed that only the hydrogenation of CO occurs, in which he proposed the trimolecular reaction of CO and molecular hydrogen to be rate determining. Leonov *et al.* (1973) were the first to model methanol synthesis kinetic over a $Cu/ZnO/Al_2O_3$ catalyst. Their model again assumed CO to be the source of carbon in methanol and did not account for the influence of CO_2 in the feed. Klier *et al.* (1982) no longer considered CO to be the only, but still the most important source of carbon in methanol. Villa *et al.* (985) realized that a thorough modelling of the methanol synthesis system should also involve a description of the gas shift reaction. Graaf *et al.* (1988, 1990) considered both the the hydrogenations of CO_2 and CO as well as the water gas shift reaction. The kinetics of low pressure methanol synthesis from CO_2, CO and H_2 on a commercial Cu/ZnO catalyst was investigated recently by Kuecha and Hoffman (1993). They stated that methanol is mainly produced from CO_2 over a deactivated catalyst. According to Lee *et al.* (1993) CO_2 is the primary source of methanol synthesis with $CO/CO_2/H_2$ feed. Methanol synthesis was much faster with CO_2/H_2 than with CO/H_2, particularly at low temperatures. Parallel to this evolution, Russian groups led by Rozovskii and Temkin (1987) developed a number of kinetic models for the SNM type $Cu/ZnO/Al_2O_3$ catalysts.

As one can see, there is still no agreement in the literature on the kinetic of methanol synthesis. The kinetics studies are often conflicting. Moreover, until now there has been no agreement as to the basic reactions occurring in the system. The role of CO_2 is insufficiently understood. It is known that some quantity of CO_2 is necessary for process to start and proceed, and many

papers indicate that methanol synthesis on copper-containing catalysts occurs not from CO, but rather via CO_2 hydrogenation.

In the current work a kinetic model for the conversion of syngas over a $Cu/ZnO/Al_2O_3$ catalyst, which is proposed by Vanden Bussche and Froment (1996), is used. Based on the results of Chinchen *et al.* (1987) and Rozovskii (1989), they assumed that CO_2 is the main source of carbon in methanol. A through description of this reaction system should also account for the water gas shift, proceeding along a redox mechanism:

$$CO + H_2O \Leftrightarrow CO_2 + H_2 \overset{+2H_2}{\Longleftrightarrow} CH_3OH + H_2O \tag{12}$$

Both reactions proceed on the copper phase of the catalyst (Chinchen *et al.*, 1987b). Finally, based upon a detailed reaction scheme derived from literature data and their own experimental work (Vanden Bussche and Froment, 1994), they developed a steady-state kinetic model for methanol synthesis and the water gas shift reaction. Unlike some other kinetic models available in the literature, this model effectively couples the rate of both overall reactions through the common surface oxygen intermediate. The following expression is obtained for the rate of methanol synthesis:

$$r_{CH_3OH} = \frac{K_D\, p_{CO_2}\, p_{H_2} \left[1 - \left(\frac{p_{H_2O}\, p_{CH_3OH}}{K^o\, p_{H_2}^3\, p_{CO_2}}\right)\right]}{(1 + K_C\, \frac{p_{H_2O}}{p_{H_2}} + K_A\, \sqrt{p_{H_2}} + K_B\, p_{H_2O})^3}, \tag{13}$$

where the equilibrium constant K^o is thermodynamically determined and the value was taken from Graaf *et al.* (1986):

$$lgK^o = \frac{3066}{T} - 10.592, \tag{14}$$

and the parameter values are given in Table 1, in which

$$K(i) = A(i)\, \exp(B(i)/RT), \tag{15}$$

where $B(i)$ represents either E or $(-\Delta H)$ or a combination of those.

All parameters are statistically significant and satisfy each of the physicochemical criteria postulated by Boudart (1972). Furthermore, the kinetic equation describe the influence of inlet temperature, pressure, and feed composition in a physically acceptable way.

K_A	A	0.499
	B	17 197
K_B	A	6.62×10^{-11}
	B	124 119
K_C	A	3 453.38
	B	-
K_D	A	1.07
	B	36 696

Table 1: Parameter values for the steady-state kinetic model (Vanden Bussche and Froment, 1996)

2.3 The ammonia and methanol synthesis reactors

Four distinct types of chemical reactors are used in the industry. These may be called batch reactors, continuous stirred-tank reactors, packed flow reactors, and unpacked flow reactors. From an analytical viewpoint, it is more convenient to group them into three classes characterized by the differential equations which describe each class. Continuous stirred tanks comprise one class. Batch reactors, packed flow reactors, and unpacked flow reactors in which fluid-dynamic effects are unimportant form a second class. The third class consists of flow reactors in which fluid-dynamic effects are important; in this class are turbulent flames, jets, and shock tubes.

Packed beds of catalyst particles is the most widely used reactor type for gas phase reactants in the chemical industry. Ammonia and methanol synthesis processes are carried out in fixed bed reactors too. In ammonia and methanol reactors the reactions, whose are autothermic, take place and they are exothermic and the elevated inlet temperature can be achieved by using the heat generated by the reaction itself. Because of thermodynamic considerations, the general requirements of reactions are that the reactants should enter the reactor at an elevated temperature and that reactions temperatures should fall as conversation proceeds. The ammonia and methanol reactors are characterized by the need to have effective cooling systems and to operate with high recycling rates. The cooling can be applied in three different ways (Dybkjaer, 1985):

— quench cooling by injection of cold syngas between adiabatic beds (e.g. ICI quench system (Macnaughtom *et al.*, 1984)),

— internal cooling with catalyst in tubes surrounded by cooling medium (e.g. Lurgi tubular packed system (Supp, 1981) or Variobar spiral-shaped boiling water tubes cooling the catalyst bed (Lahne and Lohmüller, 1986)),

— external cooling by heat exchangers between adiabatic beds (e.g.H.Topsøe (Dybkjaer, 1981), Casale mixed flow system (Smith *et al.*, 1984)).

Other variations of gas-solid ammonia and methanol reactors are fluidized bed reactors (Dry, 1988). The fluidized bed reactors have been used commercially for many highly exothermic industrial reactions of the improved heat recovery and near isothermal operation. Although these fluidized bed reactors have not been employed up to now in ammonia and methanol industry they offer attractive energy recovery and operating features, e.g. catalyst aging control by on-line catalyst removal and replenishment.

A new type of fixed-bed reactors are the axial-radial reactors. An axial-radial reactor contains one or more axial-radial beds. Part of the gas enters the catalyst bed from the top (axially), the rest through one vertical wall (radially), and all the gas leaves through the opposite wall. The main advantages of an axial-radial reactor design are a lower pressure drop than with a pure axial design and a higher catalyst utilisation than a pure radial design.

At present, the majority of commercial gas-phase catalytic processes, the ammonia and methanol synthesis being a representative example, are carried out in fixed-bed reactors. These reactors are preferred because of simpler technology and easy operation. Models employed for the process simulation and fixed-bed design can be classified into two categories: the pseudo-homogeneous and heterogeneous models. The latter distinguish between temperatures and concentrations in the bulk-gas phase and those inside the catalyst; the former do not. Each model may be one- or two-dimensional to account for gradients in radial direction perpendicular to axial flow. The basic homogeneous model usually postulates plug flow through the bed, however, it may be complicated to account for deviation from plug flow by superimposing mixing, in the axial and in special case also in radial direction (so-called dispersion). For non-isothermal situations, heat transfer has to be included in the model. In the pseudo-homogeneous model heat is considered to be transferred by the overall convection. In heterogeneous models, heat and mass transfer from the bulk to the catalyst surface is described in terms of convective mechanisms. Transport mechanisms inside the catalyst particle are expressed in terms of effective

diffusion and conduction. Because of their nature, continuum models based on effective transport mechanisms lead to differential equations. The models discussed in the current work are exclusively of the continuum type, although so-called cell models are also used for simulations of the fixed-bed reactors.

Although several reactor types are used in industry, an adiabatic quenched bed reactors are used in current work in simulations of stability of the ammonia and methanol reactors. Figure 3 represents these reactors in the simplified flow sheets with some technological parameters.

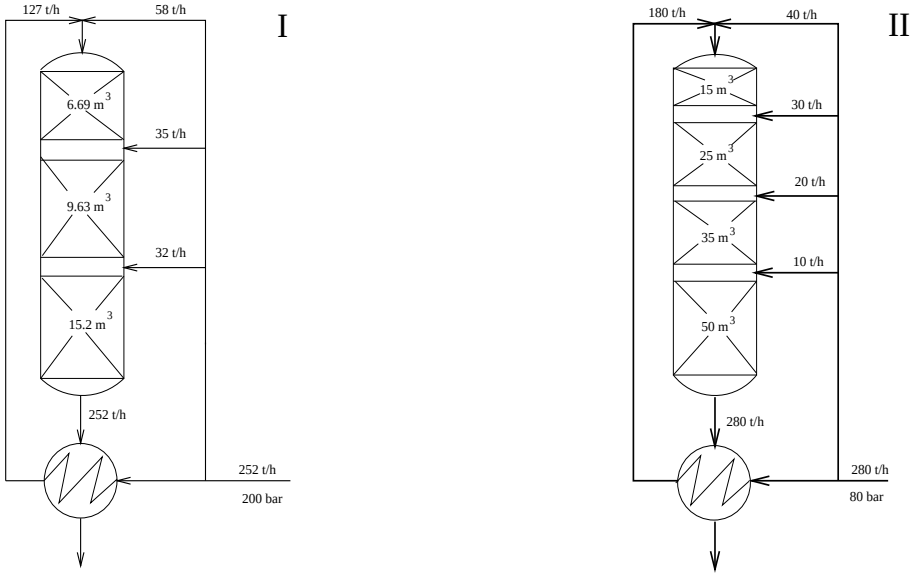

Figure 3: Simplified schemes of the ammonia and methanol synthesis reactors: I–ammonia synthesis reactor, II–methanol synthesis reactor.

Figure 3 shows that the ammonia synthesis reactor consists of three adiabatic beds and methanol synthesis reactor–of four adiabatic beds. These reactors schemes are assumed like the most usually used in industry.

3 The model and simulations

Modelling of packed bed reactors have been covered in a number of surveys: Froment (1974), Schmitz (1976), Hofmann (1979), Hlavacek and Vatruba (1977) and Hlavacek and van Rompay (1981). Although models for fixed bed reactors are abundant in the literature (see e.g. Eigenberger, 1976), the mathematical modelling for fixed bed reactors has not yet progressed as far nor been so thoroughly verified as is the case for the CSTR (Continues Stirred Tank Reactor) and the homogeneous tubular reactor. This can be ascribed to the fact that a great number of complicated process determine the behavior of this reactor type. The most important steps for model building are described by Hofman (1974). As is well known, a heterogeneous reaction on a solid catalyst takes place in several steps:

— external diffusion (reactants),

— pore diffusion (reactants),

— adsorption,

— surface reaction,

— desorption,

— pore diffusion (products),

— external diffusion (products).

In heterogeneous catalysis both thermal and kinetic instabilities can occur as a result of interaction between physical transport processes and chemical reaction. Wicke (1974) gives two examples of chemical reaction types having the properties necessary in order to exhibit kinetic instability. As one can see, based on previous works, the steady state and dynamic behavior of fixed bed reactors can be very complex even when exotic reaction rate expressions are excluded.

3.1 A simple ammonia and methanol synthesis reactors model

The main purpose of the model, which is used in simulations in the current work, is not to reproduce the industrial case with great numerical accuracy, but

rather to yield qualitative insight into the observed instability phenomenon. It is not always necessary to take all the phenomena into account and often a rather simple model can be used. In general one will choose the simplest possible model which still gives a sufficiently accurate description of the phenomena investigated. The current model for fixed bed reactor is therefore kept as simple as possible and it is taken from the study of Morud (1995).

Figure 4 indicates the simplified systems, consisting of three beds (for the ammonia synthesis reactor) and of four bed (for the methanol synthesis reactor) in series with quench using fresh feed between the beds and preheating of the feed with the effluent. For later analysis, the model of the ammonia and methanol synthesis reactor was assumed like one but different parameter values and different kinetic rate expression was used in the dynamic simulation as independent each other.

The mathematical model of the reactors consists of one model for each reactor bed. Each bed is described by a mass and energy balance in the form of two partial differential equations (see Equations 16 and 17) by discretizing the bed into ten segments. The model of the heat exchanger is lumped together with the model of the three or four reactor beds into one model. The following assumptions have been applied for each segment: axial flow only; the gas tem-

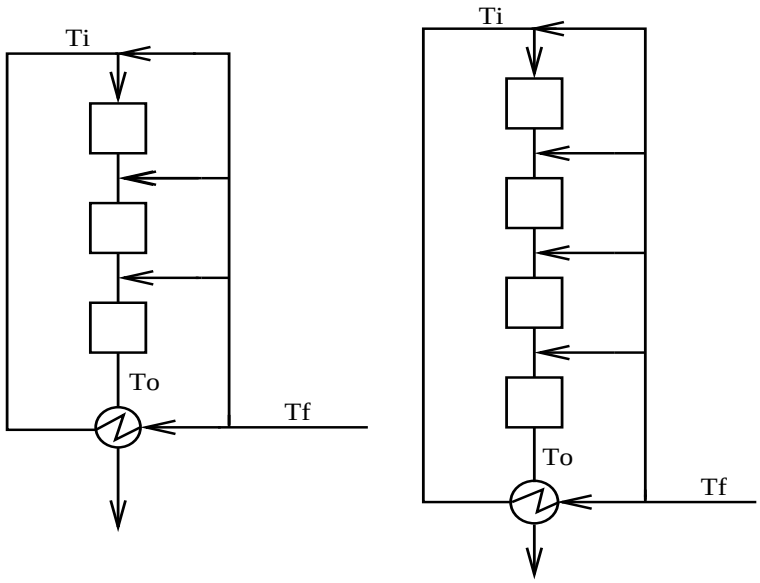

Figure 4: Sketch of reactor systems with three and four beds and preheater

perature equals the catalyst temperature; constant cross-sectional gas velocity; there is no variation in temperature, pressure and composition across the

section.

A material and energy balance yields two partial differential equations:

$$u_w \frac{\partial c}{\partial z} = \frac{C_p}{C_{pc}} r(T, c) \tag{16}$$

$$\frac{\partial T}{\partial t} + u_w \frac{\partial T}{\partial z} = \frac{-\Delta H_{rx}}{C_{pc}} r(T, c) + \Gamma \frac{\partial^2 T}{\partial z^2} \tag{17}$$

The model was discretized using a finite difference method, and integrated using a standard Runge-Kutta method. The model equations (Equation 16 and 17) may be solved as it is showed in Appendix A. The program, which is made in programming language FORTRAN 77, of dynamic simulations are presented in Appendix C.

The feed-effluent heat exchanger was modeled with an $\epsilon - NTU$ model without dynamic for simplicity. For constant flow rates this reduces to a linear relation between inlet and outlet temperatures when the fluid heat capacity is assumed to be a constant:

$$T_i = \epsilon\, T_0 + (1 - \epsilon)\, T_f, \tag{18}$$

where T_i is the reactor inlet temperature and T_0 – the reactor outlet temperature (see Figure 4) and the heat exchanger efficiency ϵ between 0 and 1 is a constant independent of temperature.

Appendix A contains others equations and numerical values for the parameters as well as a more detailed description of the model.

3.2 Linear systems and linearized model

For small deviations from the steady state, a processing unit may be well described by a linear transfer function. Before attacking the nonlinear complexities of a plant, it is therefore reasonable to review some basic results from linear systems theory.

The dynamic behavior of linear system is determined by its poles and zeros. For an uncontrolled system, the poles are the main issue, as they determine the stability of the plant. The plant is stable if and only if all the poles are in the complex left half plane. However, plant instability may not necessarily be a problem, since an unstable process may be stabilized by feedback control.

Essentially, control involves finding a way of inverting the process: one specifies the plant output, y, and the controller computes the necessary input , u, which (approximately) achieves this. With feedback control, as the bandwidth increases, the transfer function from the reference to the plant input approaches the inverse of the plant. This means that right half plane zeros in a plant would eventually end up as unstable poles in the closed loop system if the bandwidth were too high. Right half plane zeros in a plant therefore pose an upper limit to the achievable performance of any control system.

It is important to emphasize that in the current work the ammonia and methanol synthesis rectors are operated without feedback control. And later analysis provides an explanation of unstable behavior of these reactors.

For analysis, the model of ammonia and methanol synthesis reactors without the heat exchanger was linearized numerically about operating points: feed temperature 235.2 ^oC for ammonia synthesis reactor and 137.8 ^oC for methanol synthesis reactor; yielding a standard linear state space model with thirty states for ammonia synthesis reactor and forty for methanol synthesis reactor on the form:

$$\frac{dx}{dt} = A\,x + B\,u\,, \qquad y = C\,x\,, \tag{19}$$

where the state vector x consists of temperatures along the bed; u is the inlet temperature to the first bed, T_i (before the quench; quench temperature T_f was assumed constant); and y is the outlet temperature of the third bed in ammonia case and of the fourth bed in methanol case. The transfer function $g(s)$ for the reactors is then:

$$g(s) = C(cI - A)^{-1}B\,. \tag{20}$$

The model was analyzed using MATLAB. Programs in MATLAB for simulations are presented in Appendix C.

3.3 Simulations of limit cycle behavior

Simulations using the nonlinear model reproduce the observed temperature oscillations in the industrial plants and confirm that the oscillations originates in the reactor preheating systems.

A typical simulation result is shown in Figure 5, showing the inlet temperature the first reactor bed as a function of time.

In the ammonia synthesis reactor case, the system is disturbed by reducing the feed temperature, T_f, by 10 ^oC every 3000 seconds, starting from T_f=250 ^oC.

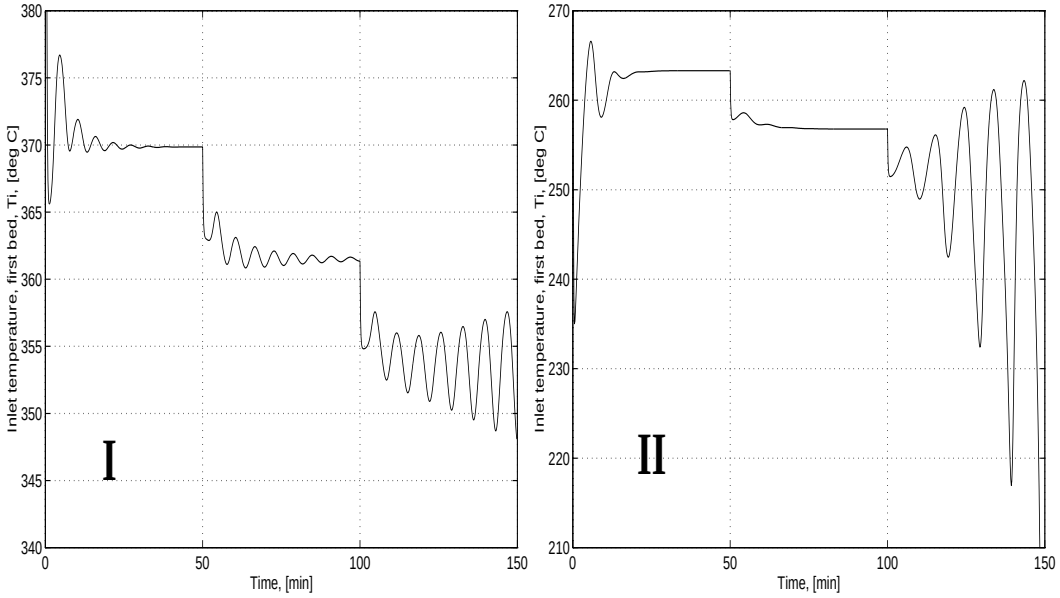

Figure 5: Stepping down the feed temperature: I–ammonia synthesis reactor, II–methanol synthesis reactor

As long as the feed temperature sufficiently high, the system is stable; however, when the feed temperature drops below some critical value ($T_{f,crit}$=235.2 ^oC), the system becomes unstable and exhibit limit cycle behavior (oscillations).

In the methanol synthesis reactor case, the system is disturbed by reducing the feed temperature, T_f, by 10 ^oC every 3000 seconds, starting from T_f=155 ^oC. The system becomes unstable like in ammonia system, when the feed temperature drops below some critical value ($T_{f,crit}$=137.8 ^oC), the system becomes unstable and exhibit limit cycle behavior (oscillations).

If the feed temperatures are kept constant after the onset of instability, the long term behavior looks like Figure 6, showing sustained oscillations in both system cases.

In both cases sustained oscillations are very similar. The ammonia reactor temperatures oscillated with 95 ^oC amplitude and the methanol reactor temperatures oscillated with 103 ^oC amplitude.

It is possible to look at the temperature of a fixed position–the first bed inlet–as

a function of time. To understand qualitatively what happens in reactors, it is considered temperature profiles through reactors at fixed times. Figures 7a to 7f show several such temperature profiles during one period of sustained oscillations in ammonia synthesis reactor. On the horizontal axis, x=0 corresponds to the inlet of the first bed and x=30 to the outlet of the last bed.

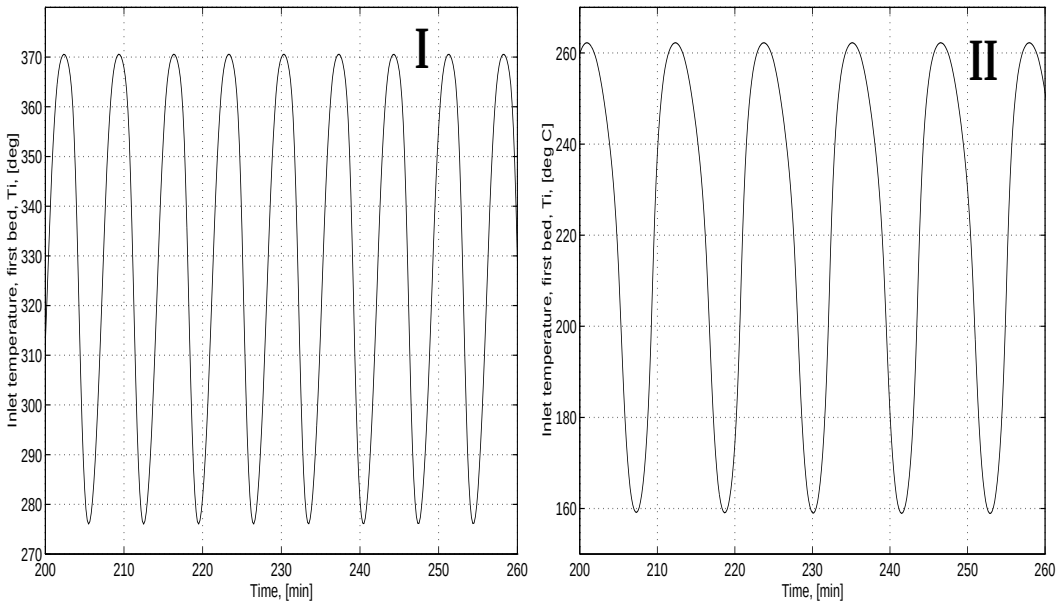

Figure 6: Sustained oscillations in temperature: I–ammonia synthesis reactor, II–methanol synthesis reactor

On the vertical axis is the reactor temperature (range 250–550 ^oC). The discontinuities in the figures are due to the quenching.

One should note the wave like bump to the left in Figure 7a. After 70 seconds, see Figure 7b, the bump has moved a little to the right, growing in size. The wave may be traced through Figures 7c–f, where it induces a new wave by heat exchange with the reactor feed, resulting in the sustained temperature oscillations.

Figures 8a to 8f show the same temperature profiles during one period of sustained oscillations in the methanol synthesis reactor. Here on the horizontal axis, x=0 corresponds to the inlet of the first bed and x=40 to the outlet of the last bed. And on the vertical axis is the reactor temperature (range 150–450 ^oC).

As one can see, the temperature profiles during one period of sustained oscillations in both reactors are very similar. It is necessary to notice that one

period of sustained oscillations in methanol synthesis reactor is 700 sec, when in ammonia synthesis rector it is 360 sec. The methanol synthesis reactor is rather inert and slower than the ammonia synthesis reactor if comparing them in kinetic schemes. This is also seen in Figure 6.

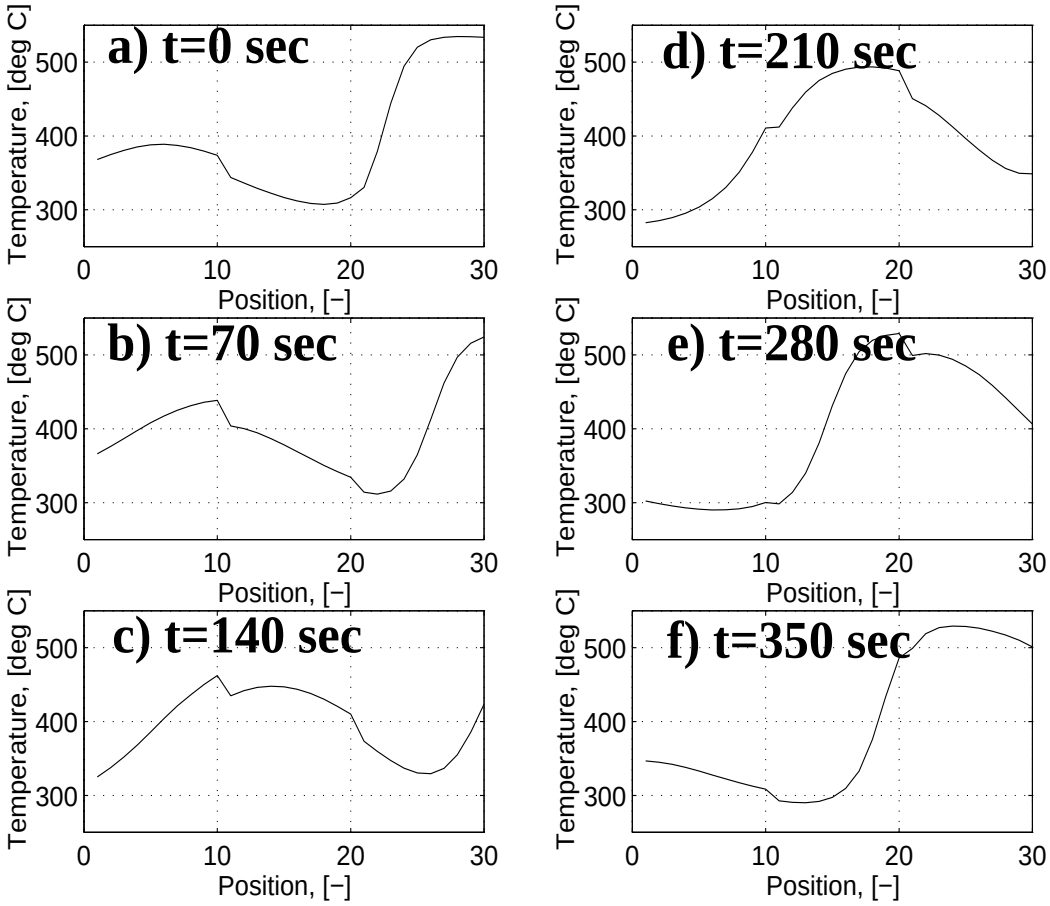

Figure 7: Sustained oscillations in the ammonia synthesis reactor

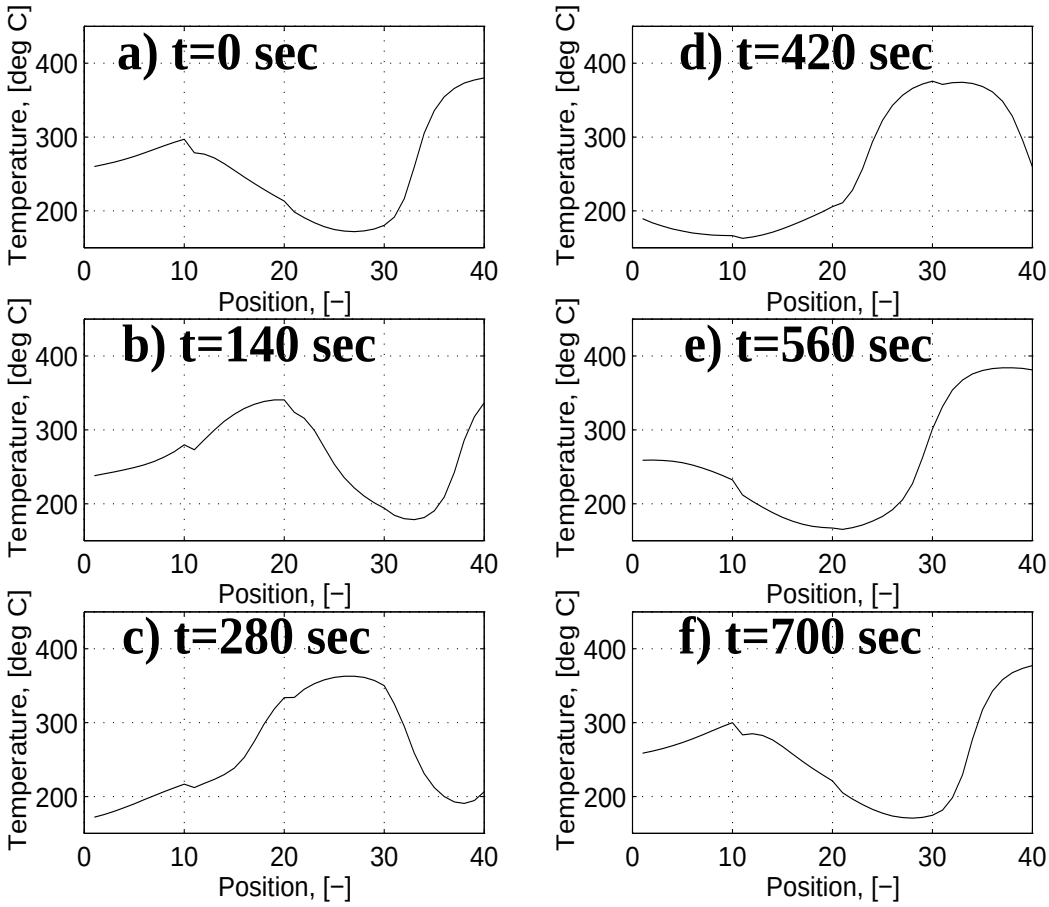

Figure 8: Sustained oscillations in the methanol synthesis reactor

4 Analysis

The objective of this section is to explain the above results. First, it can be started with a simple steady-state analysis which proves to be inadequate. Then it is performed a conventional linear stability analysis which is found to be consistent with the nonlinear simulations. Finally in the current work, it is explained why the initial steady-state analysis was inadequate in this case.

4.1 Simplified steady-state analysis

It is performed a simplified analysis based on steady-state information, similar to that of van Heerden (1953). Consider Figure 10, where the steady-state characteristic of the ammonia synthesis reactor and heat exchanger are shown. The steady-state characteristic of the methanol synthesis reactor and heat exchanger are the same; differences are only in the temperatures values, but the curves are the same form. The plot shows the relationship between the temperatures T_0 versus T_i (see Figure 4) for the ammonia synthesis reactor (S-shaped curve) and the heat exchanger (straight line). The location of S-shaped curve obviously depends on the factors that determine the kinetics of the reaction: total pressure, the reactant concentration etc. It is implicitly assumed that other quantities are held constant (flow rates, feed temperature, pressure etc.). The heat exchanger characteristic gives the relation between T_0, which is considered an input to the exchanger, and T_i, which is considered an output. Similarly, the reactor characteristic gives the relation between reactor inlet temperature, T_i, and reactor outlet temperature, T_0. S-shaped curve can also be considered as a measure of the amount of heat produced by the reaction and straight line can also considered as heat consumption in reactor, and heat exchanger system. The plot is very similar to the classical van Heerden plot (van Heerden, 1953).

Van Heerden (1953) showed that autothermic processes possess multiple steady state solutions and that under certain circumstances operation is not possible. He illustrated this by considering the heat production and consumptions curves for the very simple process. Obviously, if the overall process is adiabatic, the heat production and consumption must exactly balance each other, making the three intersections P, Q and R in Figure 9 possible steady state operating points. Van Heerden showed that P is a trivial point of no reaction, Q is unstable, since any increase in temperature will cause the heat production to be greater than the heat consumption with the result that the process moves towards R or conversely towards P for a reduction in temperature, and that

R is a stable point.

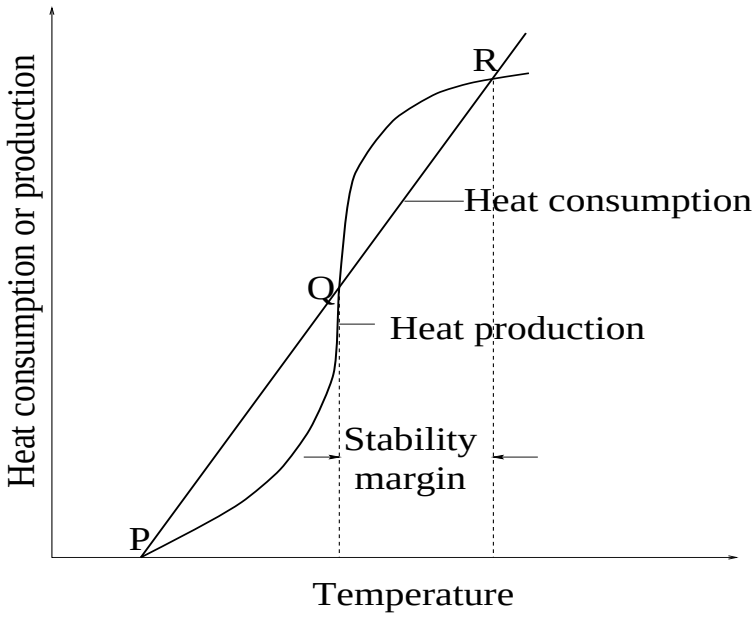

Figure 9: Heat production and consumption for the van Heerden model

By varying the plant parameters the curves can be moved relative to one another and when Q and R are coincident, the plant is on the limit of stability, any further adverse change causing the process to die.

For the conditions given in Figure 10 there are also three possible steady state solutions, and the desired one, in which is operated, is the upper one with the highest temperature. Van Heerden showed that steady states solutions where the reactor characteristic is steeper than the heat exchanger characteristic are always unstable; thus the middle solution in Figure 10 is unstable.

It is important to make a note that with control, it is possible to stabilize any operating point.

Now it can be considered the stability of the upper (desired) operating point. Van Heerden claimed that points where the heat exchanger characteristic is steeper than the reactor characteristic are stable. To induce instability one may reduce the feed temperature as done in the previous section, which corresponds closely to translating the two characteristic in Figure 10 in such a way as to bring the two curves closer to tangency (such that the middle and upper solutions coincide).

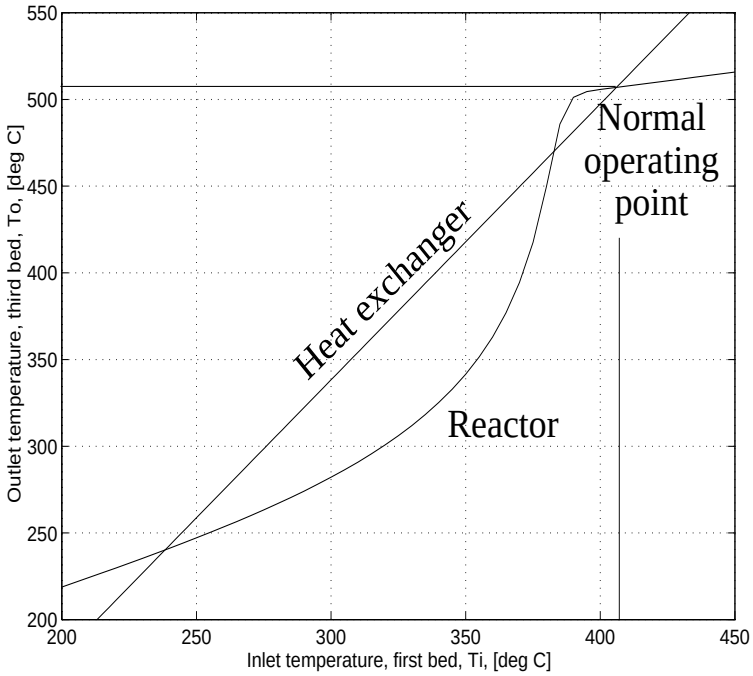

Figure 10: Steady state characteristic of reactor (S-shaped curve) and heat exchanger (straight line)

From the interpretation of van Heerden one would expect instability to occur exactly when the two curves touch each other. However, the simulations indicate that the oscillatory behavior begins just before the curves become tangents to each other. At first this was believed to be caused by nonlinearity or numerical errors, but as it is shown below a more careful analysis shows that the simulations are indeed correct, and that the upper solution may be unstable, demonstrating that a steady-state analysis is insufficient (Aris and Amundson, 1958).

4.2 Linear stability analysis

Close to an operating point, the dynamic of a system is well described by its linearized model. The reactor system, as ammonia and methanol synthesis reactors, in Figure 4 may hence be represented by the block diagram with positive feedback shown in Figure 11, where $k{=}\varepsilon$ is the steady state gain of the heat exchanger and $g(s)$ the transfer function of the reactor.

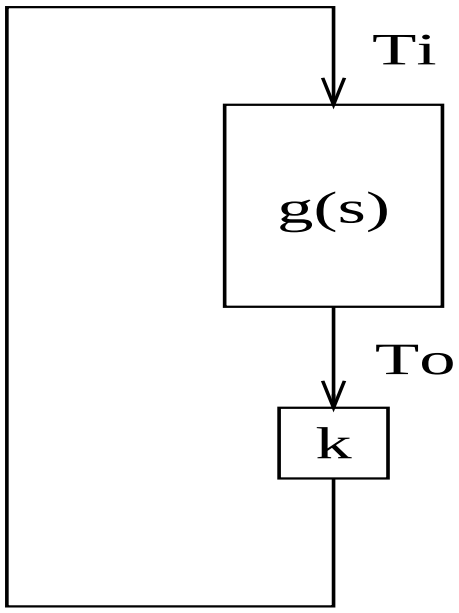

Figure 11: Block diagram

A linear stability analysis based on computing the eigenvalues (given by the zeros of $1–g(s)\,k=0$) confirmed that the instability occurred at the point found in the nonlinear simulations. Below it is considered a root locus analysis, Bode diagrams and Nyquist plots to understand what happens.

4.2.1 Analysis of reactor model

An analysis of the transfer function of $g(s)$ shows that it has several RHP (right half plane) zeros. Such RHP-zeros generally correspond to inverse responses, and this is confirmed by Figure 12 which shows the outlet temperature, T_o in response to a step increase in the inlet temperature, T_i.

In the methanol synthesis reactor case the analysis shows the same (Figure 13).

Both step responses in Figures 12 and 13 represent the response of stable linear time-invariant system, because both eventually come to finite steady-state values. In these Figures it can be seen that step responses of linearized models give reasonably good information about the amplitude rations and the range of frequencies over which disturbances can be damped by the control system. This is important question in the reactor control systems design. The

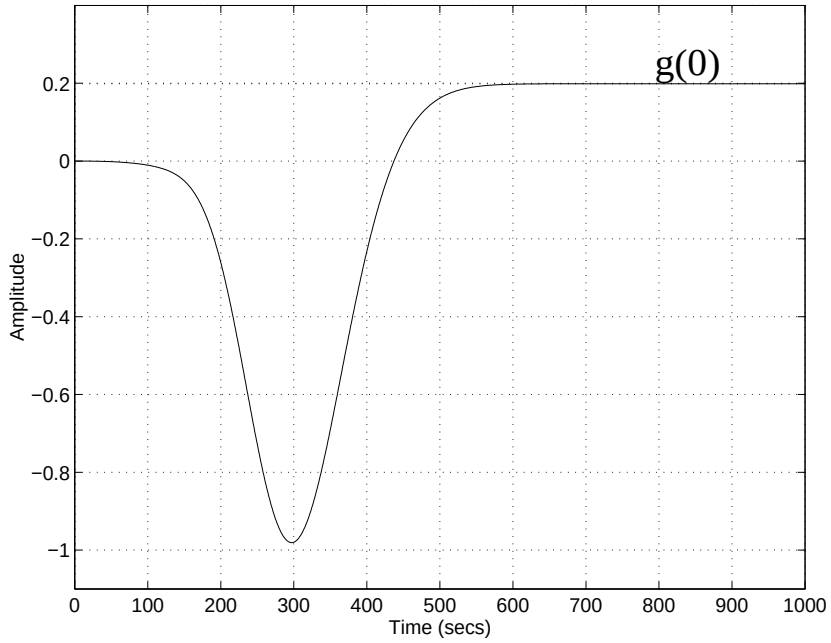

Figure 12: Step response of g(s) (reactor without preheating) for the ammonia case

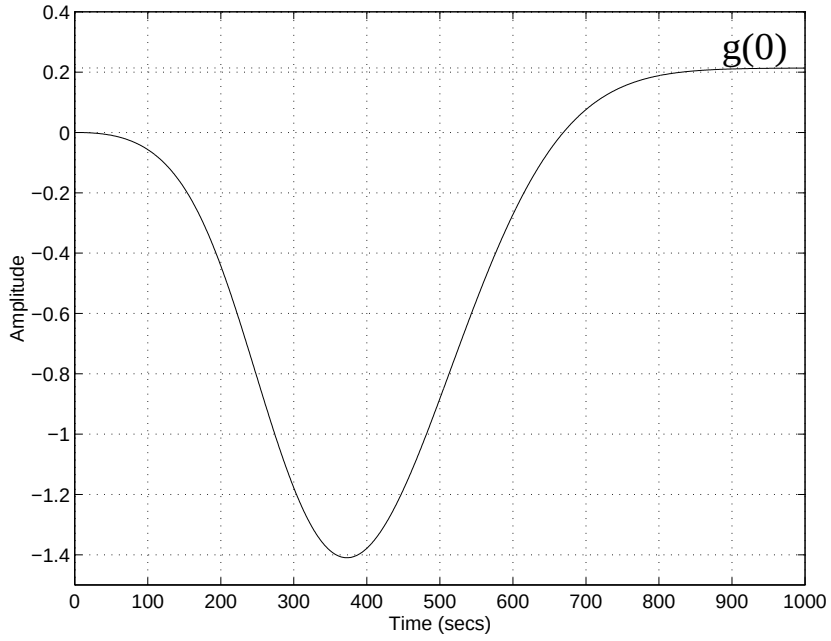

Figure 13: Step response of g(s) (reactor without preheating) for the methanol case

above responses are for the linear ammonia and methanol synthesis reactor models, and similar responses were found for the nonlinear model.

4.2.2 Root locus analysis

The root locus method was introduced by Evans (1948) and has been developed and utilized extensively in control engineering practice. It is the method for determining the locus of roots of the characteristic equation $1–g(s)\,k=0$ as k varies from zero to infinity. To see how zeros of the current transfer function affect the system stability, assume that k is varied from zero to infinity, corresponding to changing the transfer area in the heat exchanger. This yields the root locus plot shown in Figure 14. When $k=0$, the poles of the system are equal to the poles of the system without the heat exchanger (marked with 'X' on the figure). As k is increased towards infinity (corresponding to increased heat transfer area), the poles which stay finite approach the zeros of $g(s)$ (marked with 'O'). Due to the presence of the right half plane zeros, the first pole to cross the imaginary axis is not the real pole crossing the origin, but a pair of complex conjugate poles. It is also seen in Figure 15 in which is shown the root locus plot of transfer function for methanol synthesis reactor and heat exchanger system.

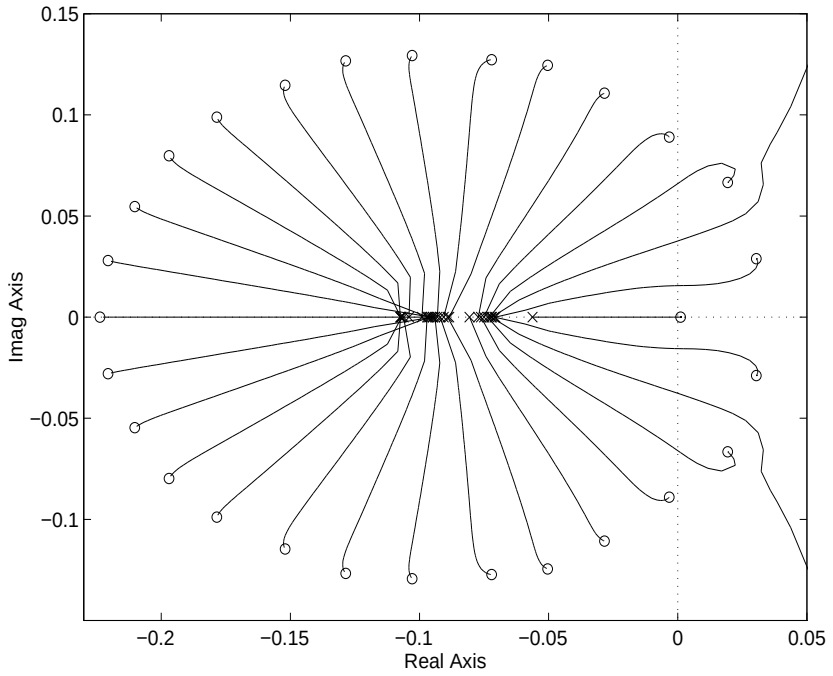

Figure 14: Root locus plot of system (the ammonia synthesis reactor case)

In both cases there are positive feedbacks ($g(0)\,k(0) > 0$). If k is varied from zero towards $1/g(0)$, $1–g(s)\,k$ approaches zero. This means that a pole goes through the origin as k passes $1/g(0)$. A pole near the origin means that the response of the plant is slow and that the sensitivity to slow disturbances is high. It is necessary to notice that it is only for most chemical engineering systems, which complex conjugate poles do not cross the imaginary axis in the root locus plot. As the gain, $|k(0)|$, is increased, the zeros of the loop gain $g(s)\,k$ attract system poles. It should be noted that because in the current case, complex conjugate poles are crossing the imaginary axis for values of k less than $1/g(0)$. In the ammonia and methanol synthesis reactors case, complex conjugate poles approaching right half plane zeros of the reactors transfer function crossed the imaginary axis for a loop gain $g(0)\,k$ less than one (Hopf bifurcation). This made reactors enter a stable limit cycle.

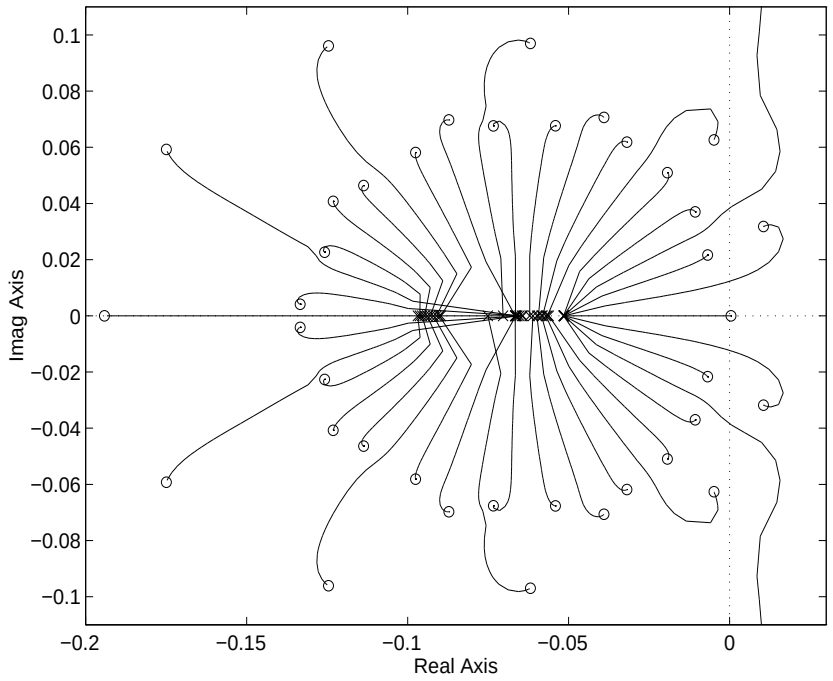

Figure 15: Root locus plot of system (the methanol synthesis reactor case)

Thus, it is not always true that positive feedback leads to slow responses and high sensitivity to disturbances, it may just as well lead to limit cycle behavior.

4.2.3 Bode diagrams analysis

The introduction of logarithmic plots, often called Bode plots, simplifies the determination of the graphical portrayal of the frequency response. The logarithmic plots are called Bode plots in honor of Bode (1945), who used them extensively in his studies of feedback amplifiers. The transfer function in the frequency domain is $g(j\omega) = |g(\omega)|e^{j\phi(\omega)}$. The logarithmic gain in decibels and the angle $\phi(\omega)$ can be plotted separately versus the frequency ω. Bode diagrams of ammonia and methanol synthesis reactors transfer functions are shown in Figure 16 and Figure 17.

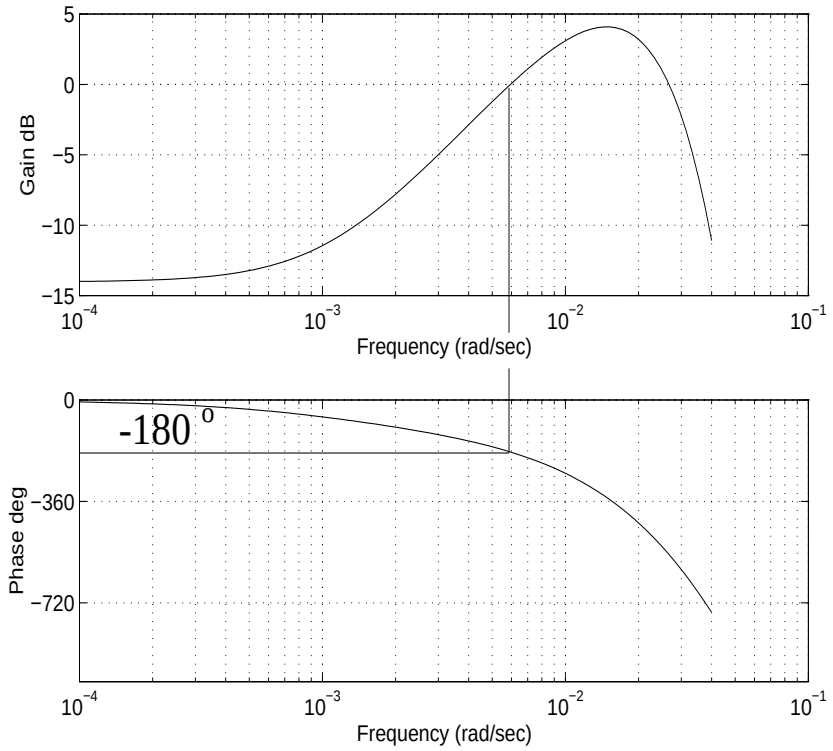

Figure 16: Bode diagrams for the ammonia synthesis reactor

The Bode magnitude plot and phase-angle plot taken together provide valuable information about closed-loop, feedback systems stability. The phase angle $\phi = -180^o$ is an important value in this regard. The output then exactly 180^o out of phase with the input signal. The closed-loop system is stable if the logarithm of the magnitude, $20\ log_{10}|g(j\omega)k|$, of the stable open-loop system is equal zero at the frequency ω at which $\phi(\omega) > -180^o$. In the case when $\phi(\omega) = -180^o$ and $20\ log_{10}|g(j\omega)k| = 0$, the closed-loop system is stable or unstable. It is the

critical point of the system. If $|g(j\omega)k| > 1$ (or 20 $log_{10}|g(j\omega)k| < 0$) at the frequency ω at which $\phi(\omega) = -180^o$, then the system is unstable in a feedback configuration. This result is a simplified statement of the important Nyquist stability theorem.

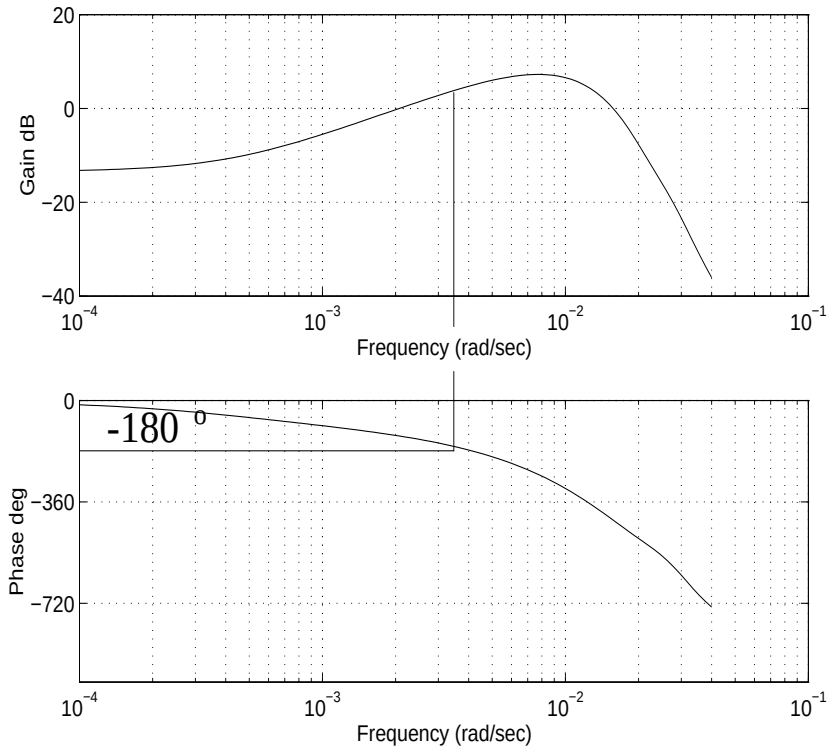

Figure 17: Bode diagrams for the methanol synthesis reactor

4.2.4 Nyquist plot analysis

The stability of the system may be analyzed using the standard Nyquist (1932) criterion: for positive feedback with a stable $g(s)$, the system is unstable if and only if a plot of the loop transfer function $g(j\omega)\,k$ encircles the $1{+}j0$ point, not $1{-}j0$ point, in the complex plane as frequency ω is varied from $-\infty$ to $+\infty$. Or, for cases in the current work: for positive feedback with a stable $g(s)$, the system is unstable if and only if a plot of the loop transfer function $g(j\omega)$ (not $g(j\omega)\,k$) encircles the $1/k{+}j0$ point, not $1/k{-}j0$ point, in the complex plane as frequency ω is varied from $-\infty$ to $+\infty$.

Consider first the stability of the middle operating point in Figure 10 (or Q point in Figure 9).

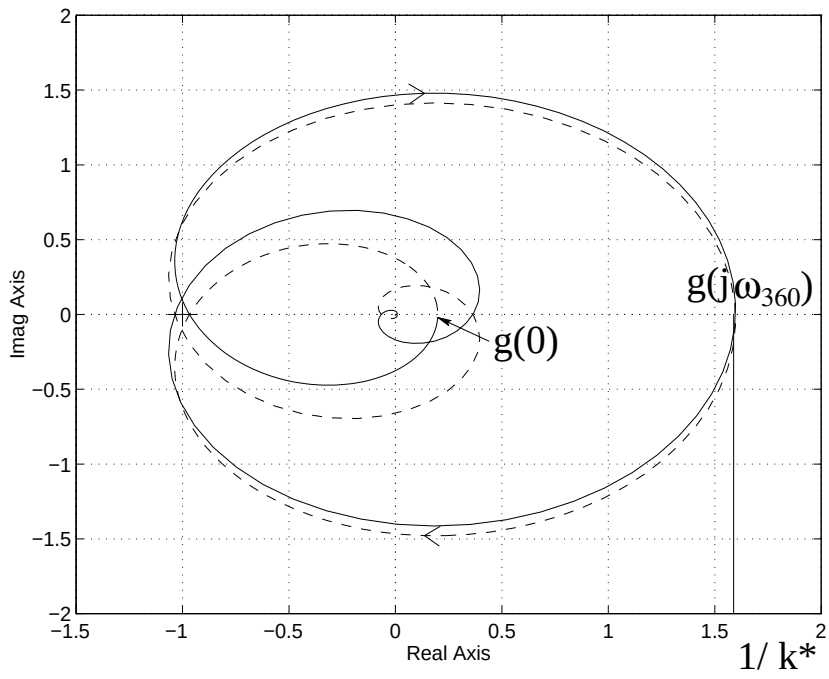

Figure 18: Nyquist plot g(s) for the ammonia synthesis reactor

The ammonia synthesis reactor steady state gain, $g(0)$, is the slope of the reactor characteristic, and the heat exchanger gain, k, is the inverse of the slope of the heat exchanger characteristic. It then follows that the steady state loop gain $g(0)\,k$ is the ratio of the two slopes, which is larger that one at this operating point since the reactor characteristic is steeper than the heat exchanger characteristic. Since $g(j\omega) = 0$ at $\omega = \pm\infty$, encirclement of the $1/k{+}j0$ point is unavoidable, and the system is therefore unstable at the middle operating point.

Normally, one will with positive feedback expect that the closed-loop system is stable when $g(0)$ is less than $1/k$. The reason is that the gain $|g(j\omega)|$ normally decreases with frequency, such that $g(j\omega)$ never cross the real axis of Nyquist plot to the right of $g(0)$ and hence never to the right of $1/k{+}j0$ point. This implies no encirclement, and thus stability of the closed-loop system. However, in the current case there are right half plane zeros in $g(s)$ which increase the loop gain and at the same time yield a negative phase shift, and make this assumption invalid. This is seen from the Nyquist plot of $g(j\omega)$ in Figure 18. There is a point of $g(j\omega)$ crossing the real axis to the right of $g(0)$ at some frequency ω_{360}. As stated above, the Nyquist stability condition tells that the system will be unstable if this curve encircles the point $1/k$. The system is stable for small values of k (corresponding to little heat integration), and

is unstable if $k > k^*$, where the critical gain k^* is given by $k^*=1/g(j\omega_{360})$. As can be seen, this gain, k^*, is a little lower than the one corresponding to the instability of the steady state, $k=1/g(0)$, i.e. the instability will occur when the heat exchanger characteristic in Figure 10 is a little steeper than the reactor characteristic. The fact that the instability occurs at a nonzero frequency, also shows that the onset of the instability corresponds to a Hopf bifurcation, which is consistent with the observed limit cycles in the nonlinear simulations.

The same analysis is done for the methanol synthesis reactor and the heat exchanger system and result was the same as can been seen in Figure 19.

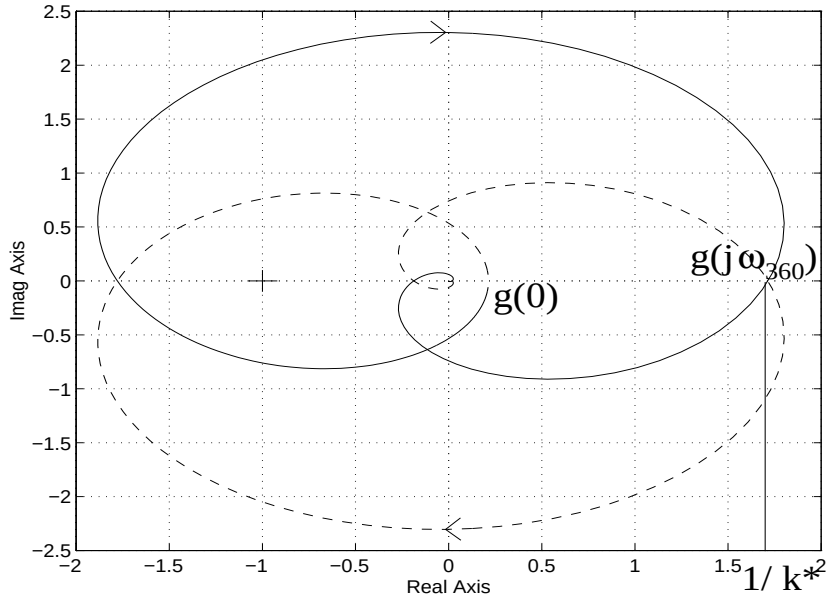

Figure 19: Nyquist plot g(s) for the methanol synthesis reactor

5 Discussion

5.1 Comparing of ammonia and methanol synthesis reactors analysis

In the current work all analysis were performed with ammonia and methanol synthesis reactors in parallels.

How it is noticed above, these reactors are very similar, because both of them are fixed bed reactors with quench cooling by injection of cold syngas between adiabatic beds. In both reactors the exothermic reactions take place. Configurations of the ammonia and methanol synthesis reactors can be various, but for the stability analysis in these studies are taken the most simple reactors used in industry and they are as close as possible. Regarding this, the stability analysis of these reactors are also get very similar. The main difference of the ammonia and methanol synthesis reactors systems are in the kinetic schemes (see Section 1.1.2). Due to the differences in the kinetic schemes, all plots of one mathematical model are not exactly the same. The one reason is that the main parameters of the reactors (gas flows, beds amount, operation conditions and etc.) are different, but it is a fact that the methanol synthesis reactor is slower than the ammonia synthesis reactor. It is seen in Figures 6, 7 and 8 and especially in Figures 12 and 13. As one can see, the overall methanol synthesis reactor response time is about 13 minutes, when for the ammonia synthesis reactor the response time is about 10 minutes. On the other hand, the methanol synthesis reactor is more sensitive than ammonia synthesis reactor in temperatures changes. This sensitiveness depends only from the kinetic processes inside reactor. In the mathematical model it is expressed in the reaction rate equations. It is very important to choose the right reaction rate expression, which is as close as possible to the industrial cases.

5.2 Explanation for the inverse response

The inverse response behavior of the ammonia and methanol synthesis reactors is shown in Figures 12 and 13. This inverse response is the main reason why reactors instability manifests themselves as oscillations and not the more common runaway without any oscillations.

As shown by Crider and Foss (1968) and Sinai and Foss (1970), an important feature of catalytic fixed bed reactor behavior is that there are two independent waves, a concentration wave and a temperature wave, which travel through the

reactor at different velocities. The concentration wave travels at approximately the chemical species velocity while the temperature wave travels at a slower velocity, which is dependent on the thermal properties of the fluid and catalyst. These waves of differing velocities are produced primarily because of the large thermal holdup in the solid phase. Due to the wave interaction, the reactor outlet temperature first decreases before it increase to a new steady state. This occurs because the step increase in the feed temperature heats the catalyst near the reactor inlet which increases the reaction rate and reduces the concentration of the fluid. Since the thermal wave velocity is less than the fluid velocity, the reactor outlet first experiences a decrease in reaction rate due to the depletion of reactant upstream. Only when the thermal wave reaches the outlet do the reaction rate and temperature start to increase. Such "wrong way" response characteristics are well known (Silverstein, 1982), and indicate right half plane zeros in the linearized transfer function of the bed. Right half plane zeros are of fundamental importance when discussing control, as they limit the achievable control performance of any control system.

5.3 Effects of other parameters in the ammonia and methanol synthesis loops

In this work, it was shown that the ammonia and methanol synthesis reactors may become unstable when the feed temperature drops below a critical value. It is very important to note that this critical value depends on some other parameters, such that instability may just as well be initiated by a sudden change one of them in the synthesis loop. The fixed-bed autothermal reactor can become less stable over time as it experiences changes in the feed pressure and concentration, the catalyst activity or the feed flow rate. Herein are given some of these parameters.

5.3.1 Effect of pressure in the synthesis loop

The pressure in the ammonia synthesis loop as well as in the methanol synthesis loop is dependent from the temperature. It is necessary to note that the pressure response in the synthesis loops is much faster than other states of the loop. The compressor characteristic is very flat, i.e. a small change in the pressure ratio results in large change in gas flow, which contributes to the numerical instability of the model. If the synthesis loop pressure is increased so the temperature of reactor increases also, because then it will make the reaction rate more high and it therefore leads the temperature to increase. On

the other hand, the increase in pressure induces a bigger gas flow and this increase requires the conformable increase in the conversation rate, which is limited by the catalyst properties. And if the catalyst activity is on the margin exploitation, in this case the temperature of reactor decreases. It is difficult to know exactly in which way temperature will change, but anyway the reactor will became unstable, if the pressure is decreased and drops below a critical value.

5.3.2 Effect of inert amount in the synthesis gas

The inert amount in the synthesis gas is regulated by the purge gas amount. The inerts increase may obtain the temperature decrease in the synthesis reactor, as the effective pressure drops and regarding this the reaction and conversation rates decrease. The reactor becomes unstable if the inerts reach the critical value. Of course, it is possible to abolish the opportunity of the reactor temperature oscillations decreasing the inerts amount. But it requires more energy consumption to decrease the inerts amount in the synthesis gas because it is not very easy to do.

5.3.3 Effect of the reaction products concentration

The startup temperature of authotermal reaction drops regarding increase reaction products concentration in the synthesis gas. If this increase is quite big, the reactor can start to extinct. The decrease of ammonia or methanol concentration induces reaction and the conversation rates. However it is not very big utility to remove completely reaction products from the synthesis gas, because it requires much energy consumption. So, the reaction products concentration in synthesis gases usually holds in the range which is more economic and is not used for the reactor stability control. Anyway, it can be the reason of the reactors instability.

5.4 Considering other ammonia and methanol reactors schemes

The stability of the ammonia or methanol synthesis reactors particular depends on which reactor schemes is used. As it is mentioned above, there is a big choice in the ammonia and methanol synthesis reactors schemes. In the current work the most usual reactors schemes in the industry were used. There are presented

some of these schemes and their stability analysis plots in Appendix B. It is possible to do inference that the transient behavior of the different reactors schemes is the same, only the critical temperature values are higher or lower.

It is important to notice that all these reactors have the same kinetic rate expressions as it is shown in Section 1.1.2. Of course, if the other kinetic expressions for the other reactor schemes are used, for example the radial or axial-radial gas streams reactors, then it is possible to achieve that reactors are stable in more extensive temperatures range than these fixed bed reactors. It can not be forgotten that reactors are without any feedback control, and if considering only the elimination of the possibility of the limit cycle behavior in reactors it is not necessary to change the reactor scheme to another. It is better to use a simple controller to do that, because it is more economic than to change whole reactor scheme.

5.5 The control of synthesis reactors

Although there has been a lot of work on the control of fixed bed reactors, many reactors in the industry are left uncontrolled. When the reactor can be operated safely without control, this is to be preferred, as it is wanted to keep the complexity of a plant to a minimum.

With the progress of control theory and especially instrumentation, the interest in handling both ammonia and methanol synthesis processes has been steadily increasing. Two important issues which have to be considered for the ammonia and methanol synthesis reactors in question are extinction and limit cycle behavior. Extinction of the reactors may occur if the reactors temperatures becomes sufficiently low. It is especially important for the methanol synthesis reactor, because it extincts at once after the limit cycle behavior and the interval of temperature from limit cycle behavior to extinction is very small. When this happens, the reactors can not resume normal operation without external addition of heat, which necessitates special startup procedures. The other important issue, limit cycle behavior induced by heat feedback through the heat exchanger, may lead to material damage in the reactors, as well as deterioration of the catalyst.

The need for a high margin of steady state stability is contrasted by the need for optimal production in the synthesis loops. Maximum production is obtained in a state where the steady-state stability margin is small. The trade off will vary according to the control of quench flow and feed gas to the reactor. Therefore the automatic control should be used in the synthesis loop. The

best philosophy is to control the inlet temperature to the reactor beds by means of the quench flow. A simple PI (Proportional-Integral) controller can be used. It is possible to use PI controller only for the quench valve before the first bed to control the temperature at the first bed inlet. Since there is no RHP zeros in this control loop, the controller is made quite fast, because the overall reactor without heat exchanger response time is about 10 minutes for ammonia case (Figure 12) and 13 minutes for methanol case (Figure 13). Thus, feedback path through the controller will dominate compared with the positive feedback through the heat exchanger, and thus the reactor with controller will behave approximately as a reactor without feed effluent heat exchange. But this controller will not eliminate the possibility of reactor extinction, which may be a big problem especially for methanol synthesis reactor. To avoid extinction, it is necessary that gas temperature at the first bed inlet is sufficiently high, with a safety margin.

Integral controls have long been used in the chemical industry to achieve the long-term maintenance of variables at the set points when the process is subjected to load disturbances.

6 Conclusions

The stability of ammonia and methanol synthesis reactors have been analyzed. The analysis have been based on the simulations for the mathematical model of reactors. The steady state behavior of reactors can be described by the classical heat production and heat removal diagram. The oscillatory behavior occurs in the simulations when the reactors feed temperature drops below a critical value. Explanation for the limit cycle behavior is the inverse response behavior of the reactors. A linear analysis close to the steady state operating point shows that instability occurs when the heat exchangers efficiency coefficient (the heat exchanger area) becomes sufficiently high. From a linear point of view, the instability may be explained using step responses, Bode diagrams, root locus and Nyquist plots techniques.

The main conclusions obtained in this thesis work are summarized as follows:

1. The stable, fixed bed ammonia and methanol synthesis reactors without any feedback control became unstable when the feed temperature drops below critical value: 235.2 ^oC for the ammonia and 137.8 ^oC for the methanol synthesis reactor.

2. The methanol synthesis reactor is slower, but more sensitive than ammonia synthesis reactor.

3. The instability of reactors depends on other operating parameters, the type of the reactor used and the synthesis loop configurations.

4. The synthesis reaction rate expression is very important to reproduce industrial reactors behavior.

5. The slow migration of temperature wave and the fast migration of concentration wave explain the inverse response behavior of reactors.

6. Due to the linear analysis, instability occurs when the heat exchanger area becomes sufficiently high.

7. The oscillatory behavior occurs as a pair of complex conjugate poles cross the imaginary axis in the complex plane.

8. The statements like "Positive feedback in a plant makes the response of the plant slow, and sensitivity to slow disturbances high" should be used with care.

9. The simple controller may eliminate the possibility of limit cycle behavior.

10. The ammonia and methanol reactors systems may undergo a Hopf bifurcation and enter a stable limit cycle for a certain change in operating parameters.

Notation

A	heat transfer area	$[m^2]$
A, B, C, D	coefficients	[-]
c	concentration	[kg/kg gas]
C_{pc}	heat capacity of catalyst and gas	[J/kg cat.K]
C_p	heat capacity of gas	[J/kg K]
C^*	ratio of flow rates	[-]
E	activation energy	[J/mol]
f	partial fugacity	[bar]
$g(s)$	transfer function	[-]
$-\Delta H_{rx}$	heat of reaction	[J/kg]
k	steady state gain	[-]
k, k_1, k_{-1}	reaction rate coefficients	[-]
K	equilibrium constant	[-]
k^*	critical gain	[-]
$\dot{m}$	mass flow rate	[kg/s]
NTU	number of transfer units	[-]
p	partial pressure	[bar]
P	pressure	[bar]
Q	heat transfer rate	[W]
r	reaction rate	[kg/kg cat.sec]
R	gas constant	[J/mol]
s	Laplase transform parameter	[-]
t	time	[sec]
T	temperature	$[\ ^oC]$
u	inlet temperature to the first bed	[-]
U	heat transfer coefficient	[W/m^2 K]
u_w	migration velocity of temperature wave	[1/sec]
x	state vector	[-]
y	outlet temperature of the last bed	[-]
z	position in reactor	[-]

Greek Symbols

ϵ	heat transfer efficiency
ρ	density
ϕ	phase angle
ω	frequency

Γ	dispersion coefficient due to finite heat transfer

Subscripts

c	cold stream
cat	catalyst
crit	critical
f	inlet gas feed
F	flow
g	gas
h	hot stream
i	inlet gas
mix	mixture
o	outlet gas
q	quench
w	wave

References

[1] Adams, R.M. and Comings, E.W. Experimental reaction rates in the synthesis of ammonia. Chem. Eng. Prog., 1953, **49**, 359.

[2] Aika, K. and Ozaki, A. Kinetics and isotope effect of ammonia synthesis over an unpromoted iron catalyst. J. Catal., 1969, **13**, 232.

[3] Aris, R. and Amundson, N.R. An analysis of chemical reactor stability and control. Chem. Eng. Sci., 1958, **7**, 3, 121.

[4] Baddour, M. Two-step catalytic reactions. AIChE J., 1972, **18**, 465.

[5] Baddour, R.F. *et al*. Steady-state simulation of an ammonia synthesis converter. Chem. Eng. Sci., 1965, **20**, 281.

[6] Barkelew, C.H. Stability of chemical reactors. Chem. Eng. Prog. Symp. Ser., 1959, **55**, 25, 37.

[7] Bode, H.W. "Network Analysis and Feedback Amplifier Design", 1945.

[8] Brill, R. Another rate equation for the catalytic synthesis of ammonia. J. Catal., 1970, **16**, 16.

[9] Chinchen, G.C. *et al*. Appl. Catal., 1987, **30**, 333.

[10] Chinchen, G.C. *et al*. Promotion of methanol synthesis and the water-gas shift reactions by adsorbed oxygen on supported copper catalysts. J. Chem. Soc., Faraday Trans. 1, 1987b, **83**, 2193.

[11] Crider, J.E. and Foss, A.S. Computational studies studies of transients in packed tubular reactors. AIChE J., 1966, **12**, 514.

[12] Crider, J.E. and Foss, A.S. An analytic solution for the dynamic of a packed adiabatic chemical reactor. AIChE J., 1968, **14**, 77.

[13] Doesburg, H. and de Jong, W.A. Transient behavior of an adiabatic fixed bed methanator. Chem. Eng. Sci., 1976, **31**, 451 and 53.

[14] Dorf, R.C. "Modern Control Systems", 1989, ISBN 0-201-14278-3.

[15] Dry, R.J. Possibilities for the development of large-capacity methanol synthesis reactors for synfuel production. Ind. Eng. Chem. Res., 1988, **27**, 616.

[16] Dybkjaer, I. Topsøe methanol technology. Chem. Econ. Eng. Rev., 1981, **13**, No6, 17.

[17] Dybkjaer, I. Desin of ammonia and methanol synthesis reactors, in ASI-NATO Chem. React. Design Technol. Conf., London Ontario, Canada, 1985, 795.

[18] Eigenberger, G. 4th ISCRE, Heidelberg, 1976.

[19] Eigenberger, G. Dynamics and stability of chemical engineering processes. Int. Ch. Eng., 1985, **25**, 4, 595.

[20] Eigenberger, G. and Schuler, H. Reactor stability and safe reaction engineering. Int. Chem. Eng., 1989, **29**, 1, 12.

[21] Evans, W.R. Graphical analysis of control systems. Transactions of the AIEE, 1948, **67**, 547.

[22] Foss, A.S. *et al*. Multivariable control system for two bed reactors by the characteristic locus method. Ind. Eng. Chem. Fund., 1980, **19**, 1, 109.

[23] Froment, G.F. Fixed bed catalytic reactors-techological and fundamental design aspects. Chem. Ing. Techn., 1974, **46**, 374.

[24] Froment, G.F. and Bischoff, K.B. "Chemical Reactor Analysis and Design". 2nd ed., Wiley, New York, 1990, 433.

[25] Gilles, E.D. Reactor models. Chem. Reaction Engng., 4th Int. Symp., Heidelberg, DECHEMA, Frankfurt, 1976, 459.

[26] Gilles, E.D. *et al*. Relaxation oscillations in chemical reactors. AIChE J., 1978, **24**, 912.

[27] Graaf, G.H. *et al*. Chemical equilibria in methanol synthesis. Chem. Eng. Sci., 1986, **41**, 2883.

[28] Graaf, G.H. *et al*. Kinetics of low-pressure methanol synthesis. Chem. Eng. Sci., 1988, **43**, 3185.

[29] Graaf, G.H. *et al*. Intra-particle diffusion limitations in low-pressure methanol synthesis. Chem. Eng. Sci., 1990, **45**, (I), 773.

[30] Gusciora, P.H. and Foss, A.S.Detecting and avoiding unstable operation of autothermal reactors. AIChE J., 1989, **35**, 6, 881.

[31] Hlavacek, V. and Votruba, J. Steady state operation of fixed-bed reactors and monolithic structures. Chem. React. Theory, 1977, 315.

[32] Hlavacek, V. and van Rompay, P. Current problems of multiplicity and sensitivity of states in chemically reacting systems. Chem. Eng. Sci., 1981, **36**, 1587.

[33] Hofmann, H. Probleme bei der mathematischen modelliering von schüttschicht-reaktoren. Chem. Ing. Techn., 1974, **46**, 236. (in German)

[34] Hofmann, H. Fortschriitte bei der modellierung von festbettreaktoren. Chem. Ing. Techn., 1979, **51**, 257. (in German)

[35] ICI: Catalyst Handbook with Special Reference to Unit Processes in Ammonia and Hydrogen Manufacture, Wolfe Scientific Books, London, 1970.

[36] Jørgensen, S.B. Fixed bed reactors dynamics and control. DYCORD-86, 1986, 11.

[37] Kiperman, V.S. and Granovskaya, V.S. Zh. Fiz. Khim., 1952, **26**, 1615.

[38] Klier, K. *et al.* Catalytic synthesis of methanol from CO/H_2, IV. The effects of carbon dioxide. J. Catal., 1982, **74**, 343.

[39] Kreith, F. and Bohn, M.S. "Principles of Heat Transfer. Harper and Row". 1986, ISBN 0-06-350369-7.

[40] Kuechen, C. and Hoffmann, U. Investigation of simultaneous reaction of carbon monoxide and carbon dioxide with hydrogen on a commercial copper/zinc oxide catalyst. Chem. Eng. Sci., 1993, **48**, 3767.

[41] Lahne, U. and Lohmüller, R. Schüttschichreaktoren mit gewickelten Kühlrhren, eine konstruktive neuentwicklung zur Durchführung exothermer katalyscher prozesse. Chem. Ing. Tech., 1986, **58**, 212. (in German)

[42] Lee, J.S. *et al.* J. Catal., 1993, **144**, 414.

[43] Leonov, V.E. *et al.* Study of the kinetics of the methanol synthesis on a low-temperature catalyst. Kinet. Katal., 1973, **14**, 848.

[44] Luss, D. and Amundson, N.R. Stability of loop reactors. AIChE J., 1967, **13**, 279.

[45] Macnaughtom, N.J. *et al.* Development of methanol technology for fuel and chemical markets. Energy Progress, 1984, **4**, 232.

[46] Morud, J.C. "Studies on the Dynamics and Operation of Integrated Plants", PhD thesis, University of Trondheim, NTH, Norway, 1995.

[47] Morud, J.C. and Skogestad, S. "The Dynamic of Chemical Reactors with Heat Integration", Paper 26e at AIChE Annual Meeting, St. Louis, USA, Nov. 8-12, 1993.

[48] Naess, L. *et al.* Using dynamic process simulation from conception to normal operation of process plants. Comp. Chem. Eng., 1992, **17**, 5/6, 585.

[49] Nata, G. in "Catalysis" (P.H.Emmet, Ed.), Reinhold, New York, 1955, **III**, 349.

[50] Nielsen, A. Review of ammonia catalysis. Catal. Rev., 1970, **4**, no.1, 1.

[51] Nusselt, W.Z. Ver. Deutch. Ing., 1927, **71**, 85.

[52] Nyquist, H. Regeneration theory. Bell System Technology J., 1932, **11**, 12.

[53] Orcutt, J.C. and Lamb, D.E. Stability of fixed-bed catalytic reactor with feed-effluent heat exchange. Autom. and Remote Contr., 1960, **4**, 274.

[54] Ozaki,A. *et al.* Proc. R. Soc. London, 1960, **A258**, 47.

[55] Pareja, G. and Reilly, M.J. Dynamic effects of recycle elements in tubular reactor systems. IEC Fund., 1969, **8**, 442.

[56] Ray, W.H. Fixed-bed reactors; dynamic and control. 2nd ISCRE, Amsterdam, 1972, A8-2.

[57] Reid, J.G. "Linear System Fundamentals", 1983, ISBN 0-07-051808-4.

[58] Reilly, M.J. and Schmitz, R.A. Dynamics of a tubular reactor with recycle: Part I. Stability of the steady state. AIChE J., 1966, **12**, 153.

[59] Reilly, M.J. and Schmitz, R.A. Dynamics of a tubular reactor with recycle: Part II. Nature of the transient state. AIChE J., 1967, **13**, 519.

[60] Rozovski, A.Ya. *et al.* React. Kinet. Katal. Lett., 1987, **34**, 87, (in Russian).

[61] Rozovski, A.Ya. Russ. Chem. Rev., 1989, **58**, 41.

[62] Schmitz, R.A. Multiplicity, stability, and sensitivity of states in chemically reacting systems-a reviews. Advan. Chem. Ser., 1975, **148**, 156.

[63] Schumann, T.E.W. J. Franklin Inst., 1929, **208**, 405.

[64] Silverstein, J.L. and Shinnar, R. Effect of design on the stability and control of fixed bed reactors with heat feedback. Ind. Eng. Chem. Proccess Des. Dev., 1982, **21**, 241.

[65] Sinai, J. and Foss, A.S. Experimental and computational studies of the dynamics of a fixed-bed chemical reactor. AIChE J., 1970, **16**, 659.

[66] Skrzypek, J. *et al.* "Methanol Synthesis", Warszawa: Polish Scientific Publ., 1994, ISBN 83-01-11490-8.

[67] Smith, R.E. *et al.* Optimize large methanol plants. Hydrocarbon Processing, 1984, **63**, (I), 95.

[68] Stephens, A.D. and Richards, R.J. Steady state and dynamic analysis of an ammonia synthesis plant. Automatica, 1973, **9**, 65-78.

[69] Supp, E. Improved methanol process. Hydrocarbon Process, 1981, 71.

[70] Temkin, M.I and Pyzhev, V. Acta Physicochim. URSS. 1940, **12**, 327.

[71] Temkin, M.I *et al.* Kinetics of ammonia synthesis far from equilibrium. Kinet. Katal., 1963, **4**, 224.

[72] Vakil, H.B. *et al.* Fixed bed reactor control with state estimation. Ind. Eng. Chem. Fund., 1973, **12**, 3, 328.

[73] Vanden Bussche, K.M. and Froment, G.F. Appl. Catal. A., 1994, **112**, 37.

[74] Vanden Bussche, K.M. and Froment, G.F. A steady-state kinetic model for methanol synthesis and the water gas shift reaction on a commercial $Cu/ZnO/Al_2O_3$ catalyst. J. Catal., 1996, **161**, 1.

[75] Van Heerden, C. Autothermic processes. Properties and reactor design. Industr. Engng. Chem. (Industr.), 1953, **45**, 1242.

[76] Villa, P. Synthesis of alcohols from carbon oxides and hydrogen. I. Kinetics of the low-pressure methanol synthesis. Ind. Eng. Chem. Proccess Des. Dev., 1985, **24**, 12.

[77] Wallmann, P.H. and Foss, A.S. Multivariable integral control for fixed bed reactors. Ind. Eng. Chem. Fund., 1979, **18**, 4, 392.

[78] Wallmann, P.H. and Foss, A.S. Experiences with dynamic estimators for fixed bed reactors. Ind. Eng. Chem. Fund., 1981, **20**, 3, 234.

[79] Wicke, E. Instabile reaktionszustände bei der heterogenen katalyse. Chem. Ing. Techn., 1974, **46**, 365. (in German)

[80] Zardi, U. Review of the developments in ammonia and methanol reactors. Hydrocarbon Processing, 1982, **8**, 129.

7 APPENDIX A. Data for the simple model

7.1 Parameters of simulation

The ammonia synthesis reactor

All ammonia reactor parameters are taken from the study of Morud (1995). The reaction is $N_2 + 3H_2 \Leftrightarrow 2NH_3$ and the feed is stoichiometric. Reaction rate is simulated by Equation 8.

Gas heat capacity, C_{pg}	3500 $J/kg\,K$
Heat capacity of catalyst, C_{pc}	1100 $J/kg\,K$
Typical operating conditions:	
Mass flow through heat exchanger, $\dot{m}_c$	127 $tons/hr$
Quench 1. bed, Q_1	58 $tons/hr$
Quench 2. bed, Q_2	35 $tons/hr$
Quench 3. bed, Q_3	32 $tons/hr$
Inlet mole fraction NH_3 (stochiometric feed)	0.04
Reactor pressure, P	200 bar
Typical inlet gas feed temperature, T_f	240 ^oC
Catalyst:	
Volume, bed 1	6.69 m^3
Volume, bed 2	9.63 m^3
Volume, bed 3	15.2 m^3
Catalyst bulk density, ρ_{cat}	2200 kg/m^3
Heat exchanger:	
Heat transfer coefficient, U	536 $W/m^2\,K$
Heat exchanger area, A	283 m^2
Calculated heat exchanger efficiency, ϵ	0.6285

The methanol synthesis reactor

The reaction is $CO + H_2O \Leftrightarrow CO_2 + H_2 \overset{+2H_2}{\Longleftrightarrow} CH_3OH + H_2O$ and the feed is stoichiometric. Reaction rate is simulated by Equation 13.

Gas heat capacity, C_{pg}	3300 $J/kg\,K$
Heat capacity of catalyst, C_{pc}	1100 $J/kg\,K$
Typical operating conditions:	
Mass flow through heat exchanger, $\dot{m}_c$	180 $tons/hr$
Quench 1. bed, Q_1	40 $tons/hr$
Quench 2. bed, Q_2	30 $tons/hr$
Quench 3. bed, Q_3	20 $tons/hr$
Quench 4. bed, Q_4	10 $tons/hr$
Inlet mole fraction CH_3OH (stochiometric feed)	0.003
Reactor pressure, P	80 bar
Typical inlet gas feed temperature, T_f	140 ^oC
Catalyst:	
Volume, bed 1	15 m^3
Volume, bed 2	25 m^3
Volume, bed 3	35 m^3
Volume, bed 4	50 m^3
Catalyst bulk density, ρ_{cat}	1150 kg/m^3
Heat exchanger:	
Heat transfer coefficient, U	550 $W/m^2\,K$
Heat exchanger area, A	390 m^2
Calculated heat exchanger efficiency, ϵ	0.6233

7.2 Mathematical model of quench points

The mixing of streams at quench points were modelled as:

$$T_{mix} = \frac{\dot{m}_F}{\dot{m}_F + \dot{m}_q} T_F + \frac{\dot{m}_q}{\dot{m}_F + \dot{m}_q} T_q \tag{21}$$

$$c_{mix} = \frac{\dot{m}_F}{\dot{m}_F + \dot{m}_q} c_F + \frac{\dot{m}_q}{\dot{m}_F + \dot{m}_q} c_q \tag{22}$$

7.3 Model for the heat exchanger

The model for the heat exchanger is a standard $\epsilon - NTU$ model for a counter current heat exchanger (see e.g. Kreith and Bohn, 1986):

$$C^* = \dot{m}_{cold}/\dot{m}_{hot} \tag{23}$$

$$NTU = \frac{UA}{\dot{m}_{cold} C_{pg}} \tag{24}$$

$$\epsilon = \frac{1 - e^{-NTU(1-C^*)}}{1 - C^* e^{-NTU(1-C^*)}} \tag{25}$$

$$Q = \epsilon \dot{m}_{cold} C_{pg} (T_{hot,in} - T_{cold,in}) \tag{26}$$

$$T_{hot,out} = T_{hot,in} - \frac{Q}{\dot{m}_{hot} C_{pg}} \tag{27}$$

$$T_{cold,out} = T_{cold,in} + \frac{Q}{\dot{m}_{hot} C_{pg}} \tag{28}$$

7.4 Numerical solution method

The model equations, Equation 16 and 17 , may be solved as follows: The reactor beds are discretized, with grid spacing Δz. First, consider the energy balance, Equation 17. This equation has the following form:

$$\frac{\partial T}{\partial t} + u_w \frac{\partial T}{\partial z} = f(T, c) + \Gamma \frac{\partial^2 T}{\partial z^2} \tag{29}$$

By Taylor series expansion to 2. order, it is got the following finite difference approximations for the space derivatives:

$$\frac{T_j - T_{j-1}}{\Delta z} = \frac{\partial T}{\partial z} - \frac{\Delta z}{2} \frac{\partial^2 T}{\partial z^2} + O(\Delta z^2) \tag{30}$$

$$\frac{T_{j+1} - 2T_j + T_{j-1}}{\Delta z^2} = \frac{\partial^2 T}{\partial z^2} + O(\Delta z^2) \tag{31}$$

Introducing these into Equation 29 yields:

$$\frac{\partial T_j}{\partial t} = f(T_j, c_j) - u_w \frac{T_j - T_{j-1}}{\Delta z} + (\Gamma - \frac{u_w \Delta z}{2}) \frac{T_{j+1} - 2T_j + T_{j-1}}{\Delta z^2} \tag{32}$$

In order not to introduce numerical instabilities, it is advisable to ensure that the coefficient of the last term stays positive:

$$\frac{\partial T_j}{\partial t} = f(T_j, c_j) - u_w \frac{T_j - T_{j-1}}{\Delta z} + max[(\Gamma - \frac{u_w \Delta z}{2}), 0] \frac{T_{j+1} - 2T_j + T_{j-1}}{\Delta z^2} \tag{33}$$

Next, consider the mass balance, Equation 16. This is an ordinary differential equation in the space coordinate, and may be integrated at a given time using whatever method, e.g. improved Euler. The system is now reduced to a system of ordinary differential equations for the temperature T_j, and may be integrated in time using any numerical method.

Improved Euler:

predictor:

$$\psi_{i,pred}^{k+1} = \psi_{i-1}^{k} + f(\psi_{i-1}^{k}) \cdot \Delta t \tag{34}$$

corrector:

$$\psi_{i}^{k+1} = \psi_{i-1}^{k} + \frac{1}{2}[f(\psi_{i-1}^{k}) + f(\psi_{i,pred}^{k+1})] \cdot \Delta t \tag{35}$$

8 APPENDIX B. Plots of various simulations

Ammonia synthesis reactor:
All parameters are the same, only heat exchanger area A=300 m^2 and Tfcrit=231.2 deg.

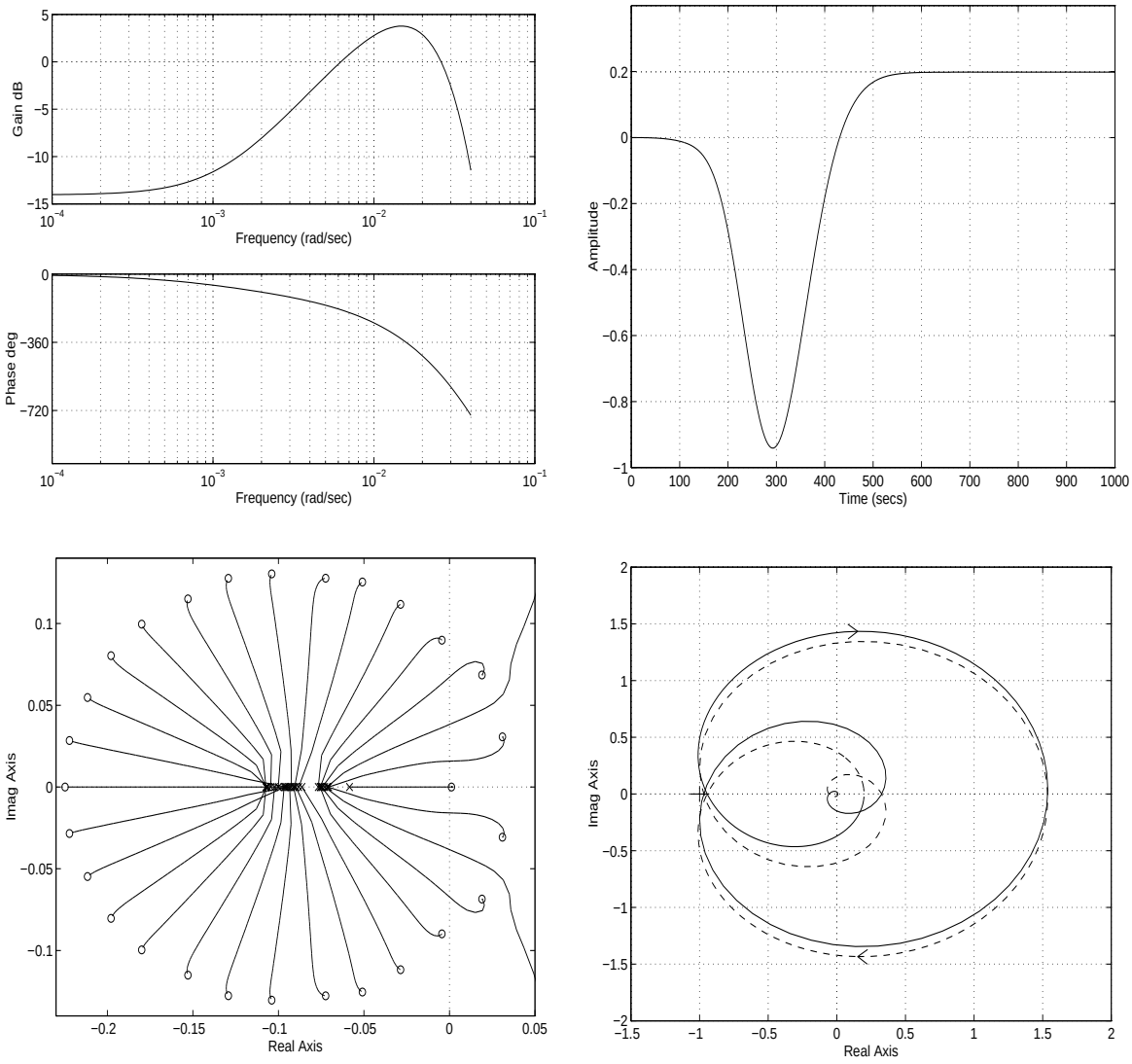

Figure 20: Ammonia synthesis reactor-2

Ammonia synthesis reactor:
All reactors parameters are the same like mentioned above, only reaction rate values are taken from industry plant (see Morud and Skogestad, 1993) and Tfcrit=234.8 deg.

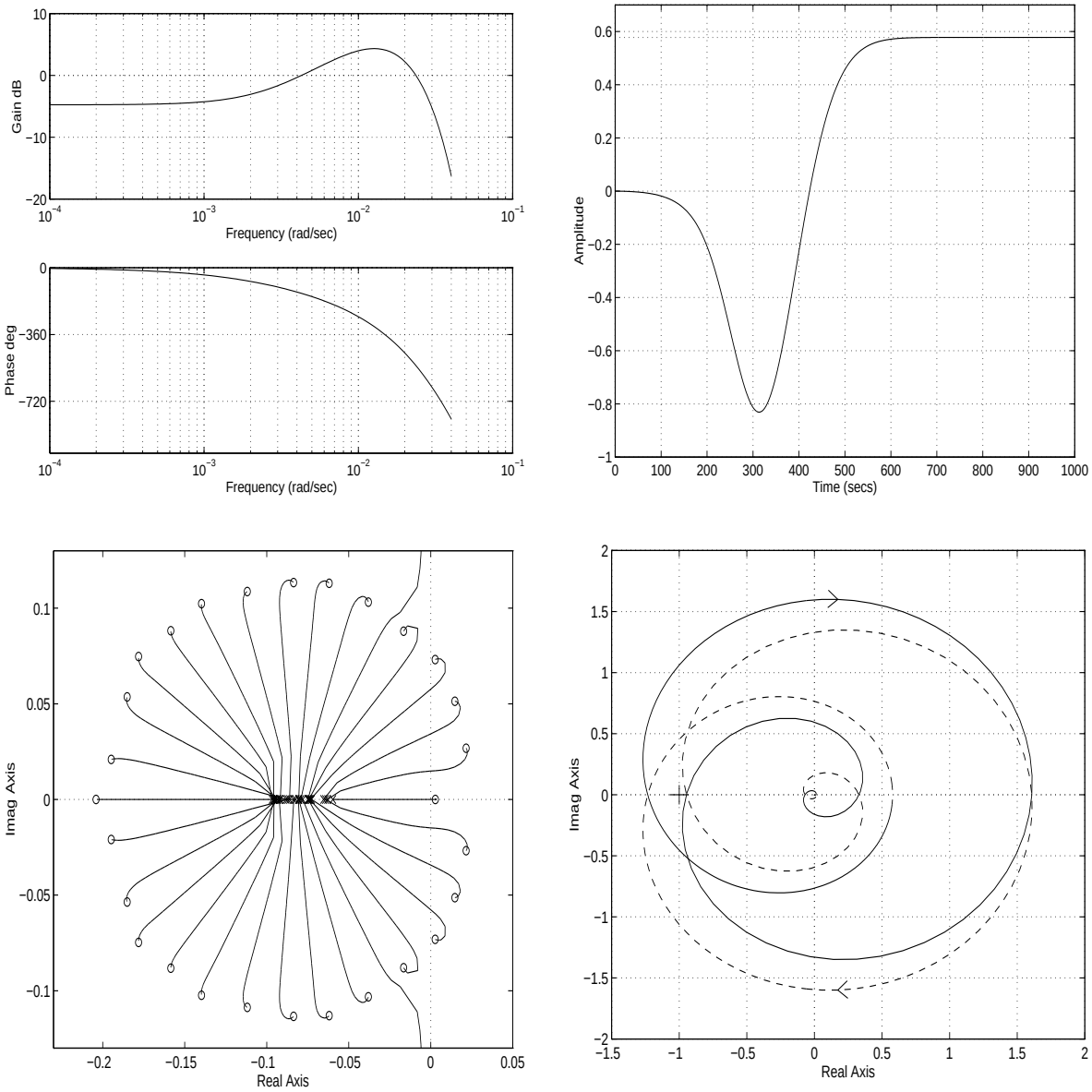

Figure 21: Ammonia synthesis reactor-3

Methanol synthesis reactor:
All reactors parameters are the same, only mc=190 t/hr and mh=200 t/hr-90 t/hr goes to another heat exchanger, then Tfcrit=155.8 deg.

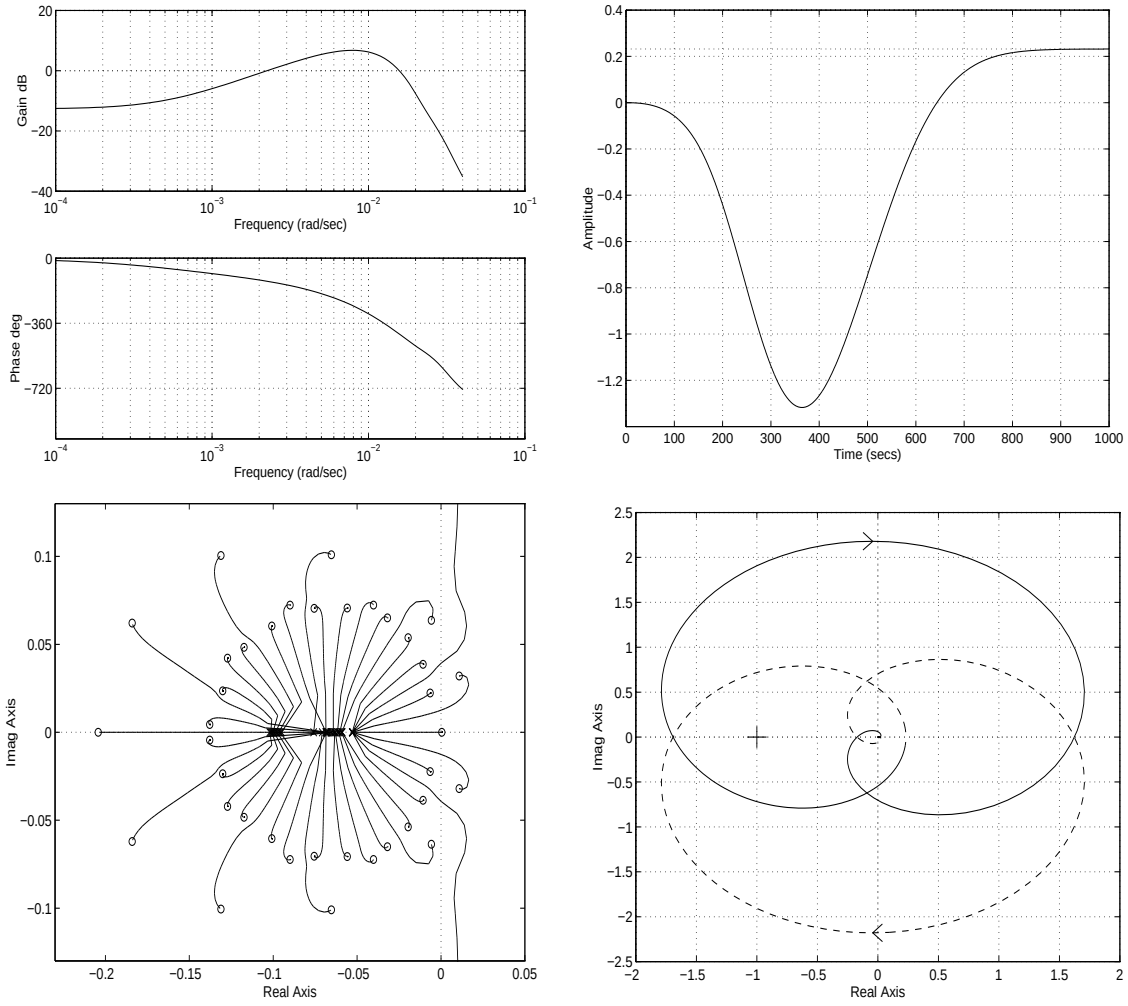

Figure 22: Methanol synthesis reactor-2

Methanol synthesis reactor:
All reactor parameters are the same, only inlet methanol concentration c=0.01, then Tfcrit=155.8 deg.

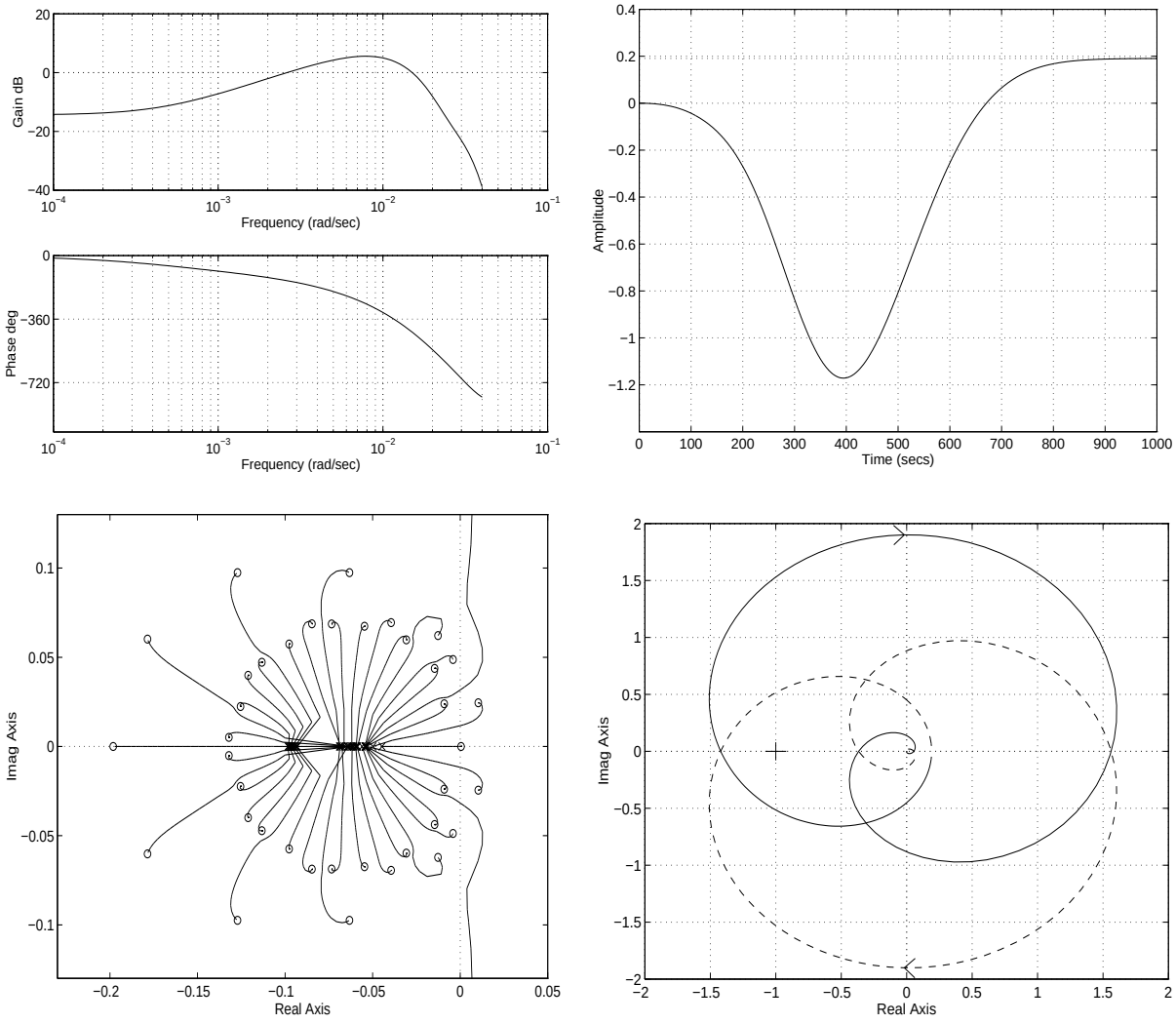

Figure 23: Methanol synthesis reactor-3

9 APPENDIX C. Programs of simulations in FORTRAN 77 and MATLAB

9.1 For the ammonia synthesis reactor

file: ammonia.f

```
      program integration
      include 'declar.f'
      real T(Npoint), dt, f(Npoint), Tp(Npoint), fp(Npoint)
      real tt, rhoc, vol1, vol2, vol3, time
      real steptime, Tfstep(10), stepindex
      integer i,j,k
      open(unit=15,file='data.m',status='new')
C  Initial parameters:
      steptime=-10.
      stepindex=1
      Tfstep(1)=250.
      Tfstep(2)=240.
      Tfstep(3)=230.
      Tfstep(4)=230.
      Tfstep(5)=230.
      Tfstep(6)=230.
      Tfstep(7)=230.
      Tfstep(8)=230.
      Tfstep(9)=230.
      Tfstep(10)=230.
      mc=127.*1000./3600.
      mh=252.*1000./3600.
      Cp=3500.
      Cpc=1100.
      Q1=58.*1000./3600.
      Q2=35.*1000./3600.
      Q3=32.*1000./3600.
      Tf=Tfstep(stepindex)
      cf=0.04
      rhoc=2200.
      vol1=6.69
      vol2=9.63
      vol3=15.2
      dHrx=2.7e6
      dm1=vol1/Nbed1*rhoc
      dm2=vol2/Nbed2*rhoc
      dm3=vol3/Nbed3*rhoc
      do 100 i=1,Npoint
        T(i)=500.
  100 continue
      dt=0.1
      do 500 k=1,10000
C Step in temperature:
      tt=100.*(k-1)*dt
      steptime=steptime+10.
      if (steptime .GE. 3000) then
        steptime=0.
        stepindex=stepindex+1
        Tf=Tfstep(stepindex)
      endif
      write(*,*) tt, T(1), T(Npoint)
```

```
C Data to file 'data.m':
      time=tt/60.
      write(15,*) 't(',k,')=',time,';'
      write(15,*) 'TT(:,',k,')=['
         do 550 i=1,Npoint
      write(15,*) T(i)
  550 continue
      write(15,*) '];'
C Start integration:
C Predictor:
      do 200 i=1,100
        call righthand(T, fp)
        do 300 j=1,Npoint
          Tp(j)=T(j)+fp(j)*dt
  300   continue
C Corrector:
        call righthand(Tp,f)
        do 400 j=1,Npoint
          T(j)=T(j)+0.5*(fp(j)+f(j))*dt
  400  continue
C End of integration:
  200  continue
  500  continue
       end

file: declar.f

       parameter (Npoint=30,Nbed1=10,Nbed2=10,Nbed3=10)
       real mc, mh, Cp, Cpc, Q1, Q2, Q3,
     & Tf, cf, dm1, dm2, dm3, dHrx
       common /crap/ mc, mh, Cp, Cpc, Q1, Q2, Q3,
     & Tf, cf, dm1, dm2, dm3, dHrx

file: righthand.f

      subroutine righthand(T,f)
      include 'declar.f'
      real T(Npoint), f(Npoint), m1, m2, m3, c(Npoint)
      real cin2, cin3, Tin1, Tin2, Tin3, dTdt(Npoint)
      integer i
      external hx, rx
      real hx, rx
C Mass Flows:
      m1=mc+Q1
      m2=m1+Q2
      m3=m2+Q3
C Concentration:
C Conc. in bed 1:
      c(1)=cf+dm1*rx(T(1),cf)/m1
      do 100 i=2,Nbed1
        c(i)=c(i-1)+dm1*rx(T(i),c(i-1))/m1
  100 continue
C Quench for bed 2:
      cin2=m1/m2*c(Nbed1)+Q2/m2*cf
C Conc. in bed 2
      c(Nbed1+1)=cin2+dm2*rx(T(Nbed1+1),cin2)/m2
      do 200 i=Nbed1+2,Nbed1+Nbed2
        c(i)=c(i-1)+dm2*rx(T(i),c(i-1))/m2
  200 continue
C Quench 3:
      cin3=m2/m3*c(Nbed2+Nbed1)+Q3/m3*cf
C Conc. in bed 3
```

```
      c(Nbed1+Nbed2+1)=cin3+dm3*rx(T(Nbed1+Nbed2+1),cin3)/m3
      do 300 i=Nbed1+Nbed2+2, Nbed1+Nbed2+Nbed3
        c(i)=c(i-1)+dm3*rx(T(i),c(i-1))/m3
  300 continue
C Temperature:
C Quench 1:
      Tin1=mc/m1*hx(T(Npoint))+Q1/m1*Tf
C dTdt in bed 1:
      dTdt(1)=(m1*Cp*(Tin1-T(1))+dm1*rx(T(1),cf)*dHrx)/(dm1*Cpc)
      do 400 i=2,Nbed1
        dTdt(i)=(m1*Cp*(T(i-1)-T(i))+dm1*rx(T(i),c(i-1))*dHrx)/(dm1*Cpc)
  400 continue
C Quench 2:
      Tin2=m1/m2*T(Nbed1)+Q2/m2*Tf
C dTdt in bed 2:
      dTdt(Nbed1+1)=(m2*Cp*(Tin2-T(Nbed1+1))
     &             +dm2*rx(T(Nbed1+1),cin2)*dHrx)/(dm2*Cpc)
      do 500 i=Nbed1+2, Nbed1+Nbed2
        dTdt(i)=(m2*Cp*(T(i-1)-T(i))
     &         +dm2*rx(T(i),c(i-1))*dHrx)/(dm2*Cpc)
  500 continue
C Quench 3:
      Tin3=m2/m3*T(Nbed1+Nbed2)+Q3/m3*Tf
C dTdt in bed 3:
      dTdt(Nbed1+Nbed2+1)=(m3*Cp*(Tin3-T(Nbed1+Nbed2+1))
     &              +dm3*rx(T(Nbed1+Nbed2+1),cin3)*dHrx)/(dm3*Cpc)
      do 600 i=Nbed1+Nbed2+2,Npoint
        dTdt(i)=(m3*Cp*(T(i-1)-T(i))
     &         +dm3*rx(T(i),c(i-1))*dHrx)/(dm3*Cpc)
  600 continue
      do 700 i=1,Npoint
        f(i)=dTdt(i)
  700 continue
      end
```

file: rate.f

```
      real function rx(T,c)
      include 'declar.f'
      real mNH3, mH2, mN2, nNH3, nH2, nN2, rate, T, c, x
      real R, p, pnh3, pn, ph, k1, k2
      mNH3=c
      mH2=(1-c)*6./34.
      mN2=(1-c)*28./34.
      nNH3=mNH3/17.
      nH2=mH2/2.
      nN2=mN2/28.
      x=nNH3/(nNH3+nH2+nN2)
      R=8.31
      p=200.
      k1=1.79E+4*exp(-87090./(R*(T+273.)))
      k2=2.57E+16*exp(-198464./(R*(T+273.)))
      pnh3=x*p
      pn=(1-x)*0.25*p
      ph=(1-x)*0.75*p
      rate=k1*pn*(ph**3/pnh3**2)**0.5 - k2*(pnh3**2/ph**3)**0.5
      rx=rate*34./2200./3600.
      rx=rx*4.75
      end
```

file: hx.f

```
      real function hx(To)
      include 'declar.f'
      real To, UA, cstar, ntu, eps, Q, Tho, Ti
      UA=536.*283.
      cstar=mc/mh
      ntu=UA/(mc*Cp)
      eps=(1-exp(-ntu*(1-cstar)))/(1-cstar*exp(-ntu*(1-cstar)))
      Q=eps*mc*Cp*(To-Tf)
      Tho=To-Q/(mh*Cp)
      Ti=Tf+Q/(mc*Cp)
      hx=Ti
      end
```

file: ammonia.m

```
clear all
global mc mh Cp Cpc Q1 Q2 Q3 Npoint Tf cf dm1 dm2 dm3 dHrx u
mc=127*1000/3600;
mh=252*1000/3600;
Cp=3500;
Cpc=1100;
Q1=58*1000/3600;
Q2=35*1000/3600;
Q3=32*1000/3600;
Npoint=30;
Tf=235.2;
cf=0.04;
rhoc=2200;
vol1=6.69;
vol2=9.63;
vol3=15.2;
dHrx=2.7e6;
dm1=vol1/Npoint*3*rhoc;
dm2=vol2/Npoint*3*rhoc;
dm3=vol3/Npoint*3*rhoc;
Tinit=400*ones(1,Npoint);
T=Tinit;
% Integration
dt=1;
for i= 1:10000
  t(i)=(i-1)*dt;
  TT(i,:)=T;
  Tpred=T+righthand(1,T)*dt;
  T=T+0.5*(righthand(1,T)+righthand(1,Tpred))*dt;
end
% Linearization
Tstasj=TT(5000,:);
delta=0.001;
for i=1:Npoint
  perturb=zeros(Npoint,1);
  perturb(i)=delta;
  A1(:,i)=(righthand(0,Tstasj+perturb')'-righthand(0,Tstasj-perturb')')/(2*delta);
end
% State characteristics of reactor
Tss=Tstasj;
 error=1;
 Tit=Tss;
 J=inv(A1);
    while error>1.e-3
    func=righthand(0,Tit);
    Tit=(Tit'-0.1*J*func')';
    error=norm(func');
```

```
  end
u=hx(Tit(Npoint),Tf);
u0=u;
norm(righthopenl(Tit));
% Open loop
Tstasj=Tit;
delta=0.001;
for i=1:Npoint
  perturb=zeros(Npoint,1);
  perturb(i)=delta;
  A1(:,i)=(righthopenl(Tstasj+perturb')'-righthopenl(Tstasj-perturb')')/(2*delta);
end
u=u0-delta;
X=righthopenl(Tstasj);
u=u0+delta;
Y=righthopenl(Tstasj);
u=u0;
B=(Y-X)/(2*delta);
B(2:Npoint)=0*B(2:Npoint);
B=B';
D=zeros(1,Npoint);
C=D;
C(Npoint)=1;
D=0;
% Plotting
om=logspace(-4,log10(0.04),100);
om2=logspace(-4,2,700);
figure(3)
bode(A1,B,C,D,1,om);
figure(4)
nyquist(A1,B,C,D,1,om2);
axis([-1.5 2 -2 2]);
grid;
figure(5)
rlocus(A1,-B,C,D);
axis([-.23 .05 -.13 .13]);
grid;
figure(6)
step(A1,B,C,D,1,1:1000);
axis([0 1000 -1 .4]);
grid;
% Steady state characteristics of reactor and exchanger
for j=1:45
  u=200+(j-1)*5;
  error=1;
  while error>1.e-3
    func=righthopenl(Tit);
    Tit=(Tit'-0.1*J*func')';
    error=norm(func);
  end
f(j)=Tit(Npoint);
zz(j)=u;
end
figure(7)
eps=0.6285;
T0=linspace(200,550,100);
Ti=eps*T0+(1-eps)*Tf;
plot(Ti,T0,zz,f);
axis([200 450 200 550]);
grid;
xlabel('Inlet temperature, first bed, Ti, [deg C]');
ylabel('Outlet temperature, third bed, To, [deg C]');
```

```
file: righthand.m

function Tprime=righthand(t,T)
global mc mh Cp Cpc Q1 Q2 Q3 Npoint Tf cf dm1 dm2 dm3 dHrx
%Mass flows:
m1=mc+Q1;
m2=m1+Q2;
m3=m2+Q3;
% Conc. in bed 1:
c(1)=cf+dm1*rx(T(1),cf)/m1;
for i=2:10
  c(i)=c(i-1)+dm1*rx(T(i),c(i-1))/m1;
end
% Quench 2:
cin2=m1/m2*c(10)+Q2/m2*cf;
% Conc. in bed 2:
c(11)=cin2+dm2*rx(T(11),cin2)/m2;
for i=12:20
  c(i)=c(i-1)+dm2*rx(T(i),c(i-1))/m2;
end
% Quench 3:
cin3=m2/m3*c(20)+Q3/m3*cf;
% Conc. in bed 3:
c(21)=cin3+dm3*rx(T(21),cin3)/m3;
for i=22:30
  c(i)=c(i-1)+dm3*rx(T(i),c(i-1))/m3;
end
% Quench 1:
Tin1=mc/m1*hx(T(30),Tf)+Q1/m1*Tf;
% dTdt in bed 1:
dTdt(1)=(m1*Cp*(Tin1-T(1))+dm1*rx(T(1),cf)*dHrx)/(dm1*Cpc);
for i=2:10
  dTdt(i)=(m1*Cp*(T(i-1)-T(i))+dm1*rx(T(i),c(i-1))*dHrx)/(dm1*Cpc);
end
% Quench 2:
Tin2=m1/m2*T(10)+Q2/m2*Tf;
% dTdt in bed 2:
dTdt(11)=(m2*Cp*(Tin2-T(11))+dm2*rx(T(11),cin2)*dHrx)/(dm2*Cpc);
for i=12:20
  dTdt(i)=(m2*Cp*(T(i-1)-T(i))+dm2*rx(T(i),c(i-1))*dHrx)/(dm2*Cpc);
end
% Quench 3:
Tin3=m2/m3*T(20)+Q3/m3*Tf;
% dTdt in bed 3:
dTdt(21)=(m3*Cp*(Tin3-T(21))+dm3*rx(T(21),cin3)*dHrx)/(dm3*Cpc);
for i=22:30
  dTdt(i)=(m3*Cp*(T(i-1)-T(i))+dm3*rx(T(i),c(i-1))*dHrx)/(dm3*Cpc);
end
Tprime=dTdt;
Tin=hx(T(Npoint),Tf);

file: righthopenl.m

function Tprime=righthopenl(T)
global mc mh Cp Cpc Q1 Q2 Q3 Npoint Tf cf dm1 dm2 dm3 dHrx
Nbed1=Npoint/3;
Nbed2=2*Nbed1;
Nbed3=Npoint;
%Mass flow:
m1=mc+Q1;
m2=m1+Q2;
```

```
m3=m2+Q3;
% Conc. in bed 1:
c(1)=cf+dm1*rx(T(1),cf)/m1;
for i=2:Nbed1
  c(i)=c(i-1)+dm1*rx(T(i),c(i-1))/m1;
end
% Quench 2:
cin2=m1/m2*c(Nbed1)+Q2/m2*cf;
% Conc. in bed 2:
c(Nbed1+1)=cin2+dm2*rx(T(Nbed1+1),cin2)/m2;
for i=Nbed1+2:Nbed2
  c(i)=c(i-1)+dm2*rx(T(i),c(i-1))/m2;
end
% Quench 3:
cin3=m2/m3*c(Nbed2)+Q3/m3*cf;
% Conc. in bed 3:
c(Nbed2+1)=cin3+dm3*rx(T(Nbed2+1),cin3)/m3;
for i=Nbed2+2:Nbed3
    c(i)=c(i-1)+dm3*rx(T(i),c(i-1))/m3;
end
% Quench 1:
Tin1=mc/m1*u+Q1/m1*Tf;
% dTdt in bed 1:
dTdt(1)=(m1*Cp*(Tin1-T(1))+dm1*rx(T(1),cf)*dHrx)/(dm1*Cpc);
for i=2:Nbed1
dTdt(i)=(m1*Cp*(T(i-1)-T(i))+dm1*rx(T(i),c(i-1))*dHrx)/(dm1*Cpc);
end
% Quench 2:
Tin2=m1/m2*T(Nbed1)+Q2/m2*Tf;
% dTdt in bed 2:
dTdt(Nbed1+1)=(m2*Cp*(Tin2-T(Nbed1+1))+dm2*rx(T(Nbed1+1),cin2)*dHrx)/(dm2*Cpc);
for i=Nbed1+2:Nbed2
  dTdt(i)=(m2*Cp*(T(i-1)-T(i))+dm2*rx(T(i),c(i-1))*dHrx)/(dm2*Cpc);
end
% Quench 3:
Tin3=m2/m3*T(Nbed2)+Q3/m3*Tf;
% dTdt in bed 3:
dTdt(Nbed2+1)=(m3*Cp*(Tin3-T(Nbed2+1))+dm3*rx(T(Nbed2+1),cin3)*dHrx)/(dm3*Cpc);
for i=Nbed2+2:Nbed3
  dTdt(i)=(m3*Cp*(T(i-1)-T(i))+dm3*rx(T(i),c(i-1))*dHrx)/(dm3*Cpc);
end
Tprime=dTdt;
```

file: rx.m

```
function r=rx(T,c)
global mc mh Cp Cpc Q1 Q2 Q3 Npoint Tf cf dm1 dm2 dm3 dHrx
mNH3=c;
mH2=(1-c)*6/34;
mN2=(1-c)*28/34;
nNH3=mNH3/17;
nH2=mH2/2;
nN2=mN2/28;
x=nNH3/(nNH3+nH2+nN2);
R=8.31;
p=200;
k1=1.79e+4*exp(-87090/(R*(T+273)));
k2=2.57e+16*exp(-198464/(R*(T+273)));
pnh3=x*p;
pn=(1-x)*0.25*p;
ph=(1-x)*0.75*p;
r=k1*pn*ph^1.5/pnh3 - k2*pnh3/ph^1.5;
```

```
r=r*34/2200/3600;
r=4.75*r;

file: hx.m

function Ti=hx(To,Tf)
global mc mh Cp
UA=536*283;
cstar=mc/mh;
ntu=UA/(mc*Cp);
epsi=(1-exp(-ntu*(1-cstar)))/(1-cstar*exp(-ntu*(1-cstar)));
Q=epsi*mc*Cp*(To-Tf);
Tho=To-Q/(mh*Cp);
Ti=Tf+Q/(mc*Cp);
```

9.2 For the methanol synthesis reactor

```
file: methanol.f

      program integration
      include 'mdeclar.f'
      real T(Npoint), dt, f(Npoint), Tp(Npoint), fp(Npoint)
      real tt, rhoc, vol1, vol2, vol3, vol4, time
      real steptime, Tfstep(10), stepindex
      integer i,j,k
      open(unit=15,file='data.m',status='new')
C  intial  parameters:
      steptime=-10.
      stepindex=1
      Tfstep(1)=155.
      Tfstep(2)=145.
      Tfstep(3)=135.
      Tfstep(4)=135.
      Tfstep(5)=135.
      Tfstep(6)=135.
      Tfstep(7)=135.
      Tfstep(8)=135.
      Tfstep(9)=135.
      Tfstep(10)=135.
      mc=180.*1000./3600.
      mh=280.*1000./3600.
      Cp=3300.
      Cpc=1100.
      Q1=40.*1000./3600.
      Q2=30.*1000./3600.
      Q3=20.*1000./3600.
      Q4=10.*1000./3600.
      Tf=Tfstep(stepindex)
      cf=0.003
      rhoc=1150.
      vol1=15.
      vol2=25.
      vol3=35.
      vol4=50.
      dHrx=5.e7
      dm1=vol1/Nbed1*rhoc
      dm2=vol2/Nbed2*rhoc
      dm3=vol3/Nbed3*rhoc
      dm4=vol4/Nbed4*rhoc
```

```
C reaction beginner temperature:
      do 100 i=1,Npoint
        T(i)=270.
  100 continue
      dt=0.1
      do 500 k=1,10000
C step in time:
      tt=100.*(k-1)*dt
      steptime=steptime+10.
      if (steptime .GE. 3000) then
        steptime=0.
        stepindex=stepindex+1
        Tf=Tfstep(stepindex)
      endif
      write(*,*) tt, T(1), T(Npoint)
c Data to file:'mdata.m'
      time=tt/60
      write(15,*) 't(',k,')=',time,';'
      write(15,*) 'TT(:,',k,')=['
         do 550 i=1,Npoint
      write(15,*) T(i)
  550 continue
      write(15,*) '];'
C start of integration:
C Predictor:
      do 400 i=1,100
        call mrighthand(T, fp)
        do 300 j=1,Npoint
          Tp(j)=T(j)+fp(j)*dt
  300   continue
C Corrector:
       call mrighthand(Tp,f)
       do 200 j=1,Npoint
         T(j)=T(j)+0.5*(fp(j)+f(j))*dt
  200  continue
C End of integration:
  400  continue
  500  continue
       end

file: mdeclar.f

       parameter (Npoint=40,Nbed1=10,Nbed2=10,Nbed3=10,Nbed4=10)
       real mc,mh,Cp,Cpc,Q1,Q2,Q3,Q4,Tf,cf,dm1,dm2,dm3,dm4,dHrx
       common /crap/ mc,mh,Cp,Cpc,Tf,Q1,Q2,Q3,Q4,cf,dm1,dm2,dm3,dm4,dHrx

file: mrighthand.f

      subroutine mrighthand(T,f)
      include 'mdeclar.f'
      real T(Npoint), f(Npoint),m1,m2,m3,m4,c(Npoint)
      real cin2,cin3,cin4,Tin1,Tin2,Tin3,Tin4,dTdt(Npoint)
      integer i
      external mhx, mrx
      real mhx, mrx
C   Flows:
      m1=mc+Q1
      m2=m1+Q2
      m3=m2+Q3
      m4=m3+Q4
C Concentration in bed 1:
      c(1)=cf+dm1*mrx(T(1),cf)/m1
```

```
      do 100 i=2,10
        c(i)=c(i-1)+dm1*mrx(T(i),c(i-1))/m1
  100 continue
C Quench for bed 2:
      cin2=m1/m2*c(10)+Q2/m2*cf
C Concentration in bed 2:
       c(11)=cin2+dm2*mrx(T(11),cin2)/m2
       do 200 i=12,20
        c(i)=c(i-1)+dm2*mrx(T(i),c(i-1))/m2
  200 continue
C Quench for bed 3:
      cin3=m2/m3*c(20)+Q3/m3*cf
C Concentration in bed 3:
      c(21)=cin3+dm3*mrx(T(21),cin3)/m3
      do 300 i=22,30
        c(i)=c(i-1)+dm3*mrx(T(i),c(i-1))/m3
  300 continue
C Quench for bed 4:
      cin4=m3/m4*c(30)+Q4/m4*cf
C Concentration in bed 4:
      c(31)=cin4+dm4*mrx(T(31),cin4)/m4
      do 400 i=32,Npoint
        c(i)=c(i-1)+dm4*mrx(T(i),c(i-1))/m4
  400 continue
C Quench 1:
      Tin1=mc/m1*mhx(T(Npoint))+Q1/m1*Tf
C dTdt in bed 1:
      dTdt(1)=(m1*Cp*(Tin1-T(1))+dm1*mrx(T(1),cf)*dHrx)/(dm1*Cpc)
      do 500 i=2,Nbed1
       dTdt(i)=(m1*Cp*(T(i-1)-T(i))+dm1*mrx(T(i),c(i-1))*dHrx)/(dm1*Cpc)
  500 continue
C Quench 2:
      Tin2=m1/m2*T(10)+Q2/m2*Tf
C dTdt in bed 2:
      dTdt(11)=(m2*Cp*(Tin2-T(11))+dm2*mrx(T(11),cin2)*dHrx)/(dm2*Cpc)
      do 600 i=12, 20
        dTdt(i)=(m2*Cp*(T(i-1)-T(i))+dm2*mrx(T(i),c(i-1))*dHrx)/(dm2*Cpc)
  600 continue
C Quench 3:
      Tin3=m2/m3*T(20)+Q3/m3*Tf
C dTdt in bed 3:
      dTdt(21)=(m3*Cp*(Tin3-T(21))+dm3*mrx(T(21),cin3)*dHrx)/(dm3*Cpc)
      do 700 i=22,30
        dTdt(i)=(m3*Cp*(T(i-1)-T(i))+dm3*mrx(T(i),c(i-1))*dHrx)/(dm3*Cpc)
  700 continue
C Quench 4:
      Tin4=m3/m4*T(30)+Q4/m4*Tf
C dTdt in bed 4:
      dTdt(31)=(m4*Cp*(Tin4-T(31))+dm4*mrx(T(31),cin4)*dHrx)/(dm4*Cpc)
      do 800 i=32,Npoint
        dTdt(i)=(m4*Cp*(T(i-1)-T(i))+dm4*mrx(T(i),c(i-1))*dHrx)/(dm4*Cpc)
  800 continue
      do 900 i=1,Npoint
        f(i)=dTdt(i)
  900 continue
      end

file: mrate.f

      real function mrx(T,c)
      include 'mdeclar.f'
      real T,c,x,mCH3OH,mCO2,mH2,mH2O,nCH3OH,nCO2,nH2,nH2O
```

```
      real p,pch3oh,pco2,ph2,ph2o,lgK0,K0,R
      real A(4),B(4),K(4),r,r1,r2
      integer i
      mCH3OH=c
      mCO2=(1-c)*44./32.
      mH2=(1-c)*6./32.
      mH2O=(1-c)*18./32.
      nCH3OH=mCH3OH/32.
      nCO2=mCO2/44.
      nH2=mH2/2.
      nH2O=mH2O/18.
      x=nCH3OH/(nCH3OH+nCO2+nH2+nH2O)
      p=80.
      pch3oh=x*p
      pco2=(1-x)*p*0.2
      ph2=(1-x)*p*0.6
      ph2o=(1-x)*p*0.2
      lgK0=(3066./(T+273))-10.592
      K0=10.**lgK0
      R=8.314
      A(1)=0.499
      B(1)=17197.
      A(2)=6.62E-11
      B(2)=124119.
      A(3)=3453.38
      B(3)=0.
      A(4)=1.07
      B(4)=36696.
      do 100 i=1,4
         K(i)=A(i)*exp(B(i)/(R*(T+273)))
 100  continue
      r1=K(4)*pco2*ph2*(1-ph2o*pch3oh/(K0*ph2**3*pco2))
      r2=(1+K(3)*ph2o/ph2+K(1)*sqrt(ph2)+K(2)*ph2o)**3
c mol/kgcat/s
      r=r1/r2
C kg/kgcat/s
      mrx=r*32./1000.
      end

file: mhx.f

      real function mhx(To)
      include 'mdeclar.f'
      real To, UA, cstar, ntu, eps, Q, Ti
      UA=550.*390.
      cstar=mc/mh
      ntu=UA/(mc*Cp)
      eps=(1-exp(-ntu*(1-cstar)))/(1-cstar*exp(-ntu*(1-cstar)))
      Q=eps*mc*Cp*(To-Tf)
      Ti=Tf+Q/(mc*Cp)
      mhx=Ti
      end

file: methanol.m

clear all
global mc mh Cp Cpc Q1 Q2 Q3 Q4 Npoint Tf cf dm1 dm2 dm3 dm4 dHrx u
mc=180*1000/3600;
mh=280*1000/3600;
Cpc=1100;
Q1=40*1000/3600;
Q2=30*1000/3600;
```

```
Q3=20*1000/3600;
Q4=10*1000/3600;
Npoint=40;
cf=0.003;
rhoc=1150;
vol1=15;
vol2=25;
vol3=35;
vol4=50;
dm1=vol1/Npoint*4*rhoc;
dm2=vol2/Npoint*4*rhoc;
dm3=vol3/Npoint*4*rhoc;
dm4=vol4/Npoint*4*rhoc;
Cp=3300;
dHrx=5e7;
Tf=137.8;
Tinit=270*ones(1,Npoint);
T=Tinit;
% Integration
dt=1;
for i= 1:10000
  t(i)=(i-1)*dt;
  TT(i,:)=T;
  Tpred=T+mrighthand(1,T)*dt;
  T=T+0.5*(mrighthand(1,T)+mrighthand(1,Tpred))*dt;
%Linearization
Tstasj=TT(5000,:);
delta=0.001;
for i=1:Npoint
  perturb=zeros(Npoint,1);
  perturb(i)=delta;
  A1(:,i)=(mrighthand(0,Tstasj+perturb')'-mrighthand(0,Tstasj-perturb')')/(2*delta);
end
% State characteristics of reactor
Tss=Tstasj;
 error=1;
 Tit=Tss;
 J=inv(A1);
    while error>1.e-3
    func=mrighthand(0,Tit);
    Tit=(Tit'-0.1 *J*func')';
    error=norm(func');
  end
u=mhx(Tit(Npoint),Tf);
u0=u;
norm(mrighthopenl(Tit));
end
% Open loop
Tstasj=Tit;
delta=0.001;
for i=1:Npoint
  perturb=zeros(Npoint,1);
  perturb(i)=delta;
  A1(:,i)=(mrighthopenl(Tstasj+perturb')'-mrighthopenl(Tstasj-perturb')')/(2*delta);
  i
end
u=u0-delta;
X=mrighthopenl(Tstasj);
u=u0+delta;
Y=mrighthopenl(Tstasj);
u=u0;
B=(Y-X)/(2*delta);
```

```
B(2:Npoint)=0*B(2:Npoint);
B=B';
D=zeros(1,Npoint);
C=D;
C(Npoint)=1;
D=0;
% Plotting
om=logspace(-4,log10(0.04),100);
om2=logspace(-4,2,700);
figure(3)
bode(A1,B,C,D,1,om);
figure(4)
nyquist(A1,B,C,D,1,om2);
grid;
axis([-2. 2 -2.5 2.5]);
grid;
figure(5)
rlocus(A1,-B,C,D);
axis([-.2 .03 -.11 .11]);
figure(6)
step(A1,B,C,D,1,1:1000);
axis([0 1000 -1.5 .4]);
grid;
```

file: mrighthand.m

```
function Tprime=mrighthand(t,T)
global mc mh Cp Cpc Q1 Q2 Q3 Q4 Npoint Tf cf dm1 dm2 dm3 dm4 dHrx
%Mass flows:
m1=mc+Q1;
m2=m1+Q2;
m3=m2+Q3;
m4=m3+Q4;
Nb=Npoint/4;
% Conc. in bed 1:
c(1)=cf+dm1*mrx(T(1),cf)/m1;
for i=2:(Nb)
  c(i)=c(i-1)+dm1*mrx(T(i),c(i-1))/m1;
end
% Quench  2:
cin2=m1/m2*c(Nb)+Q2/m2*cf;
% Conc. in bed 2
c(Nb+1)=cin2+dm2*mrx(T(Nb+1),cin2)/m2;
for i=(Nb+2):(2*Nb)
  c(i)=c(i-1)+dm2*mrx(T(i),c(i-1))/m2;
end
% Quench 3:
cin3=m2/m3*c(2*Nb)+Q3/m3*cf;
% Conc. in bed 3
c(2*Nb+1)=cin3+dm3*mrx(T(2*Nb+1),cin3)/m3;
for i=(2*Nb+2):(3*Nb)
    c(i)=c(i-1)+dm3*mrx(T(i),c(i-1))/m3;
end
% Quench 4:
cin4=m3/m4*c(3*Nb)+Q4/m4*cf;
% Conc.  in bed 4
c(3*Nb+1)=cin4+dm4*mrx(T(3*Nb+1),cin4)/m4;
for i=(3*Nb+2):Npoint
    c(i)=c(i-1)+dm4*mrx(T(i),c(i-1))/m4;
end
% Quench 1:
Tin1=mc/m1*mhx(T(Npoint),Tf)+Q1/m1*Tf;
```

```
% dTdt in bed 1:
dTdt(1)=(m1*Cp*(Tin1-T(1))+dm1*mrx(T(1),cf)*dHrx)/(dm1*Cpc);
for i=2:Nb
  dTdt(i)=(m1*Cp*(T(i-1)-T(i))+dm1*mrx(T(i),c(i-1))*dHrx)/(dm1*Cpc);
end
% Quench 2:
Tin2=m1/m2*T(Nb)+Q2/m2*Tf;
% dTdt in bed 2:
dTdt(Nb+1)=(m2*Cp*(Tin2-T(Nb+1))+dm2*mrx(T(Nb+1),cin2)*dHrx)/(dm2*Cpc);
for i=Nb+2:2*Nb
  dTdt(i)=(m2*Cp*(T(i-1)-T(i))+dm2*mrx(T(i),c(i-1))*dHrx)/(dm2*Cpc);
end
% Quench 3:
Tin3=m2/m3*T(2*Nb)+Q3/m3*Tf;
% dTdt in bed 3:
dTdt(2*Nb+1)=(m3*Cp*(Tin3-T(2*Nb+1))+dm3*mrx(T(2*Nb+1),cin3)*dHrx)/(dm3*Cpc);
for i=2*Nb+2:3*Nb
  dTdt(i)=(m3*Cp*(T(i-1)-T(i))+dm3*mrx(T(i),c(i-1))*dHrx)/(dm3*Cpc);
end
% Quench 4:
Tin4=m3/m4*T(3*Nb)+Q4/m4*Tf;
% dTdt in bed 4:
dTdt(3*Nb+1)=(m4*Cp*(Tin4-T(3*Nb+1))+dm4*mrx(T(3*Nb+1),cin4)*dHrx)/(dm4*Cpc);
for i=3*Nb+2:Npoint
  dTdt(i)=(m4*Cp*(T(i-1)-T(i))+dm4*mrx(T(i),c(i-1))*dHrx)/(dm4*Cpc);
end
Tprime=dTdt;

file: mrighthopenl.m

function Tprime=mrighthopenl(T)
global mc mh Cp Cpc Q1 Q2 Q3 Q4 Npoint Tf cf dm1 dm2 dm3 dm4 dHrx u
Nbed1=Npoint/4;
Nbed2=2*Nbed1;
Nbed3=3*Nbed1;
Nbed4=Npoint;
%flows:
m1=mc+Q1;
m2=m1+Q2;
m3=m2+Q3;
m4=m3+Q4;
%Conc. in bed 1:
c(1)=cf+dm1*mrx(T(1),cf)/m1;
for i=2:Nbed1
  c(i)=c(i-1)+dm1*mrx(T(i),c(i-1))/m1;
end
% Quench  2:
cin2=m1/m2*c(Nbed1)+Q2/m2*cf;
%Conc. in bed 2:
c(Nbed1+1)=cin2+dm2*mrx(T(Nbed1+1),cin2)/m2;
for i=Nbed1+2:Nbed2
  c(i)=c(i-1)+dm2*mrx(T(i),c(i-1))/m2;
end
% Quench 3:
cin3=m2/m3*c(Nbed2)+Q3/m3*cf;
%Conc. in bed 3:
c(Nbed2+1)=cin3+dm3*mrx(T(Nbed2+1),cin3)/m3;
for i=Nbed2+2:Nbed3
  c(i)=c(i-1)+dm3*mrx(T(i),c(i-1))/m3;
end
% Quench 4:
cin4=m3/m4*c(Nbed3)+Q4/m4*cf;
```

```
%Conc. in bed 4:
c(Nbed3+1)=cin4+dm4*mrx(T(Nbed3+1),cin4)/m4;
for i=Nbed3+2:Nbed4
  c(i)=c(i-1)+dm4*mrx(T(i),c(i-1))/m4;
end
% Quench 1:
Tin1=mc/m1*u+Q1/m1*Tf;
% dTdt in bed 1:
dTdt(1)=(m1*Cp*(Tin1-T(1))+dm1*mrx(T(1),cf)*dHrx)/(dm1*Cpc);
for i=2:Nbed1
  dTdt(i)=(m1*Cp*(T(i-1)-T(i))+dm1*mrx(T(i),c(i-1))*dHrx)/(dm1*Cpc);
end
% Quench 2:
Tin2=m1/m2*T(Nbed1)+Q2/m2*Tf;
% dTdt in bed 2:
dTdt(Nbed1+1)=(m2*Cp*(Tin2-T(Nbed1+1))+dm2*mrx(T(Nbed1+1),cin2)*dHrx)/(dm2*Cpc);
for i=Nbed1+2:Nbed2
  dTdt(i)=(m2*Cp*(T(i-1)-T(i))+dm2*mrx(T(i),c(i-1))*dHrx)/(dm2*Cpc);
end
% Quench 3:
Tin3=m2/m3*T(Nbed2)+Q3/m3*Tf;
% dTdt in bed 3:
dTdt(Nbed2+1)=(m3*Cp*(Tin3-T(Nbed2+1))+dm3*mrx(T(Nbed2+1),cin3)*dHrx)/(dm3*Cpc);
for i=Nbed2+2:Nbed3
  dTdt(i)=(m3*Cp*(T(i-1)-T(i))+dm3*mrx(T(i),c(i-1))*dHrx)/(dm3*Cpc);
end
% Quench 4:
Tin4=m3/m4*T(Nbed3)+Q4/m4*Tf;
% dTdt in bed 4:
dTdt(Nbed3+1)=(m4*Cp*(Tin4-T(Nbed3+1))+dm4*mrx(T(Nbed3+1),cin4)*dHrx)/(dm4*Cpc);
for i=Nbed3+2:Nbed4
  dTdt(i)=(m4*Cp*(T(i-1)-T(i))+dm4*mrx(T(i),c(i-1))*dHrx)/(dm4*Cpc);
end
Tprime=dTdt;
```

file: mrx.m

```
function r=mrx(T,c)
mCH3OH=c;
mCO2=(1-c)*44/32;
mH2=(1-c)*6/32;
mH2O=(1-c)*18/32;
nCH3OH=mCH3OH/32;
nCO2=mCO2/44;
nH2=mH2/2;
nH2O=mH2O/18;
x=nCH3OH/(nCH3OH+nCO2+nH2+nH2O);
p=80;
pch3oh=x*p;
pco2=(1-x)*p*0.2;
ph2=(1-x)*p*0.6;
ph2o=(1-x)*p*0.2;
lgK0=(3066/(T+273))-10.592;
K0=10^lgK0;
R=8.314;
A(1)=0.499;
B(1)=17197;
A(2)=6.62e-11;
B(2)=124119;
A(3)=3453.38;
B(3)=0;
A(4)=1.07;
```

```
B(4)=36696;
for i=1:4
 K(i)=A(i)*exp(B(i)/(R*(T+273)));
end
r1=K(4)*pco2*ph2*(1-ph2o*pch3oh/(K0*ph2^3*pco2));
r2=(1+K(3)*ph2o/ph2+K(1)*sqrt(ph2)+K(2)*ph2o)^3;
% mol/kgcat/s
r=r1/r2;
% kg/kgcat/s;
r=r*32/1000;
```

file: mhx.m

```
function Ti=mhx(To,Tf)
global mc mh Cp
UA=550*390;
cstar=mc/mh;
ntu=UA/(mc*Cp);
epsi=(1-exp(-ntu*(1-cstar)))/(1-cstar*exp(-ntu*(1-cstar)));
Q=epsi*mc*Cp*(To-Tf);
Tho=To-Q/(mh*Cp);
Ti=Tf+Q/(mc*Cp);
```